Centro Fermi
Museo Storico della Fisica e
Centro Studi e Ricerche Enrico Fermi

ICORE : Innovative COating REsearch

Innocenzo M. Pinto

University of Sannio, INFN, LVC and KAGRA

Rome, IT, March 2, 2016

Outlook

Why Coating R&D

Where are we now : the aLIGO mirrors

How can we progress:

- Improving Modeling
- Improving Processes
- Improving Characterization

Ongoing Studies & New Ideas:

- Nanolayered Composites
- Silicon Nitrides
- Crystalline Coatings
- M-ary Coatings
- Metamaterial Coatings

Conclusions

GW150914, 1st Detected GW

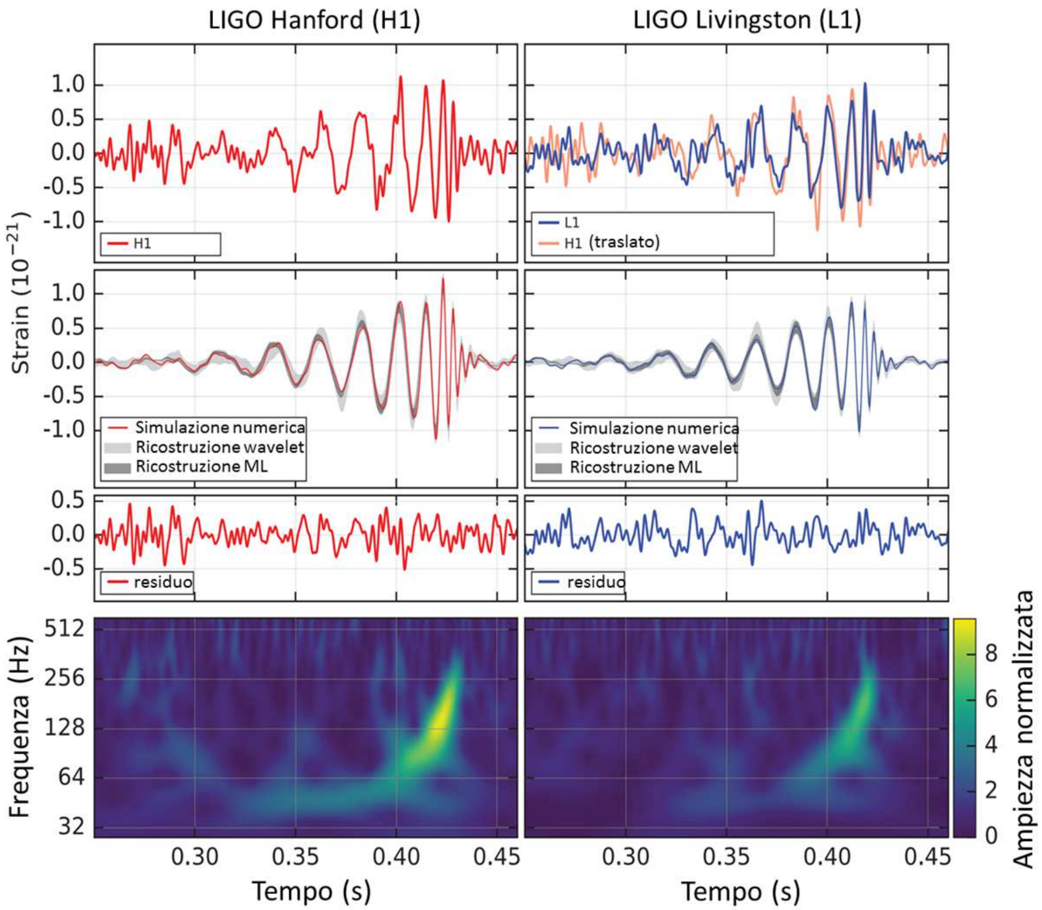

	Valore stimato	Unitá
M_1	36^{+5}_{-4}	$M_\odot$
M_1	29^{+4}_{-4}	$M_\odot$
M_{fin}	62^{+4}_{-4}	$M_\odot$
s	$0.67^{+0.05}_{-0.07}$	-
R_L	410^{+160}_{-180}	Mpc
z	$0.09^{+0.03}_{-0.04}$	-

Expected Pay-offs : Astrophysics

Observation of GW from extreme – mass – ratio - inspirals (EMRI) allows mapping the spacetime geometry [J.R. Gair et Al., Phys. Rev. D77 (2008) 024 035] around a collapsed galactic core (*holiodesy*)

Gravitational radiation from spinning neutron stars (pulsars), and neutron-star binaries in their merger phase will bring signatures of the equation of state of nuclear star matter [J. S. Read et al., Phys.Rev. D79 (2009) 124033], and indicate whether strange (quark) particles or exotic phase transitions are involved;

Reconstructing the mass multipoles of the collapsed cores from the observed waveforms, it will be possible to check the black hole "no-hair" theorem [L. Barack and C. Cutler, Phys. Rev. D75 (2007) 042003]

Compact binary systems in their inspiral (pre-coalescence) phase are standard candles of gravitational light, whose observation will permit to measure Hubble's recession to an unprecedented degree of accuracy [S. Capozziello, Astroparticle Physics, 33 (2010) 190]

The *Big Ears* (as of 2017)

Interferometric Detectors

Effect of monochromatic GW
(+ polarization, normal incidence)
on a planar ring of freely-falling
test particles

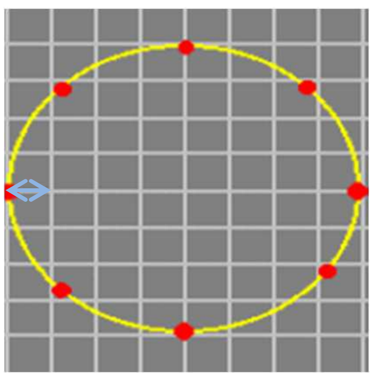

$\Delta\ell$

ℓ

Tidal force: $\Delta\ell \propto \ell$

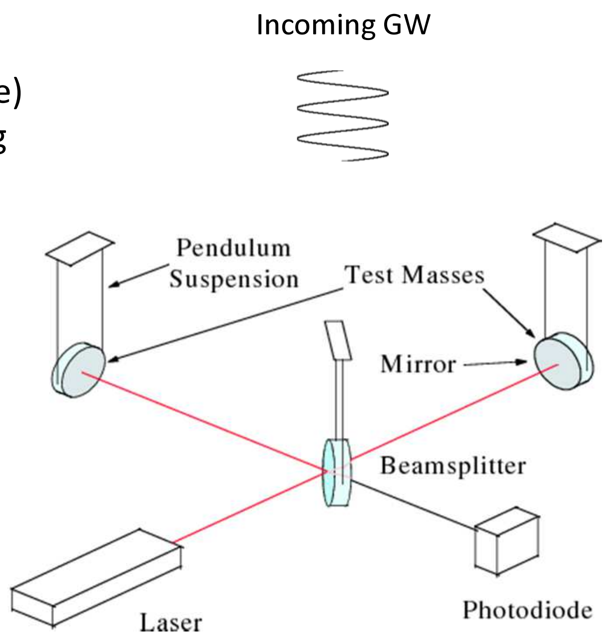

A bare-bone interferometric
detector of GW

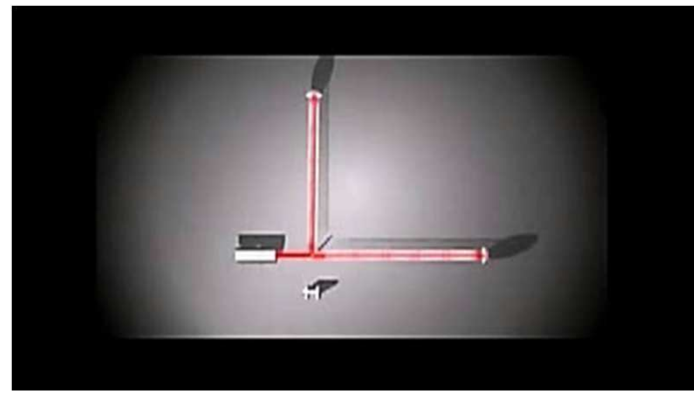

… transforms the GW into an
electric signal (antenna = transducer)

Typical wave *strength* : $h \cong \Delta\ell / \ell \approx 10^{-26} \div 10^{-19}$ - ***Very weak !!!***

aLIGO Noise Budget

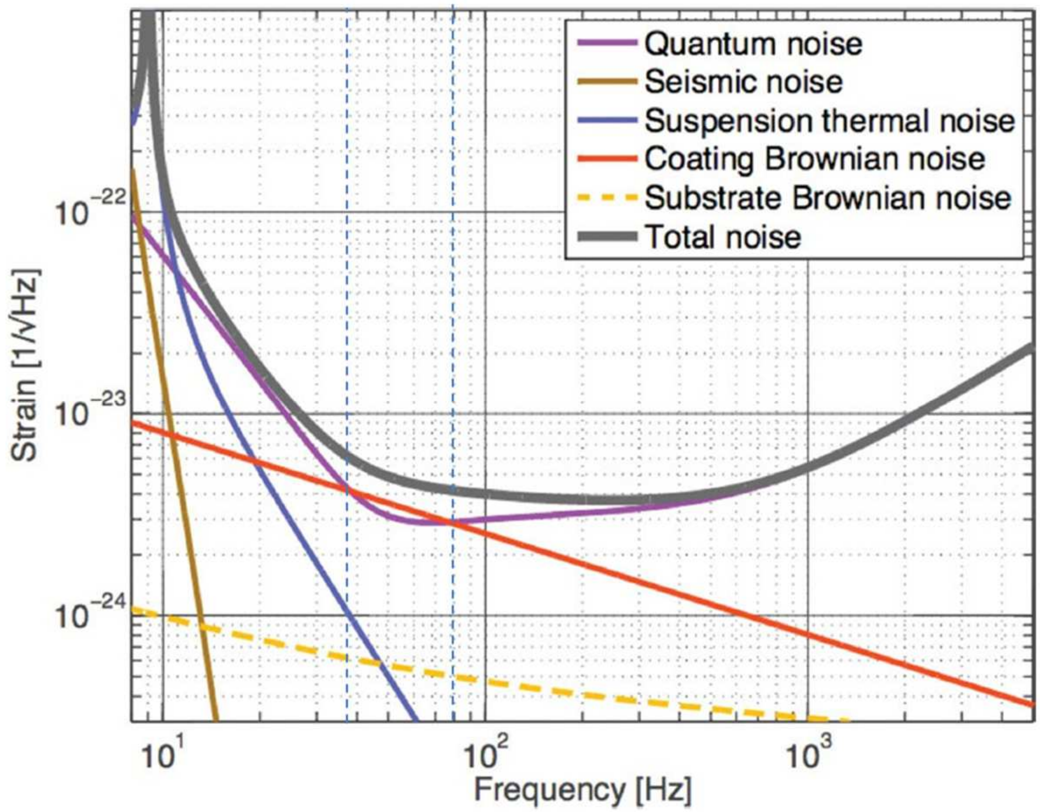

[Waldman, LIGO P0900115]

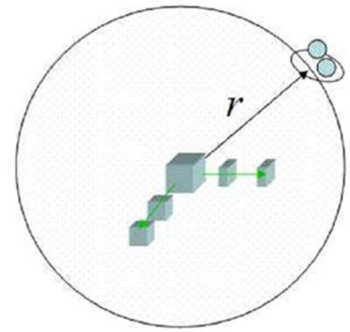

Visibility volume & event rate $\propto PSD_{floor}^{-3/2}$

... a $\mathbf{5\mu m}$ thick film sets the performance of a $\mathbf{5Km}$ size detector !!

GW150914, 1st Detected GW

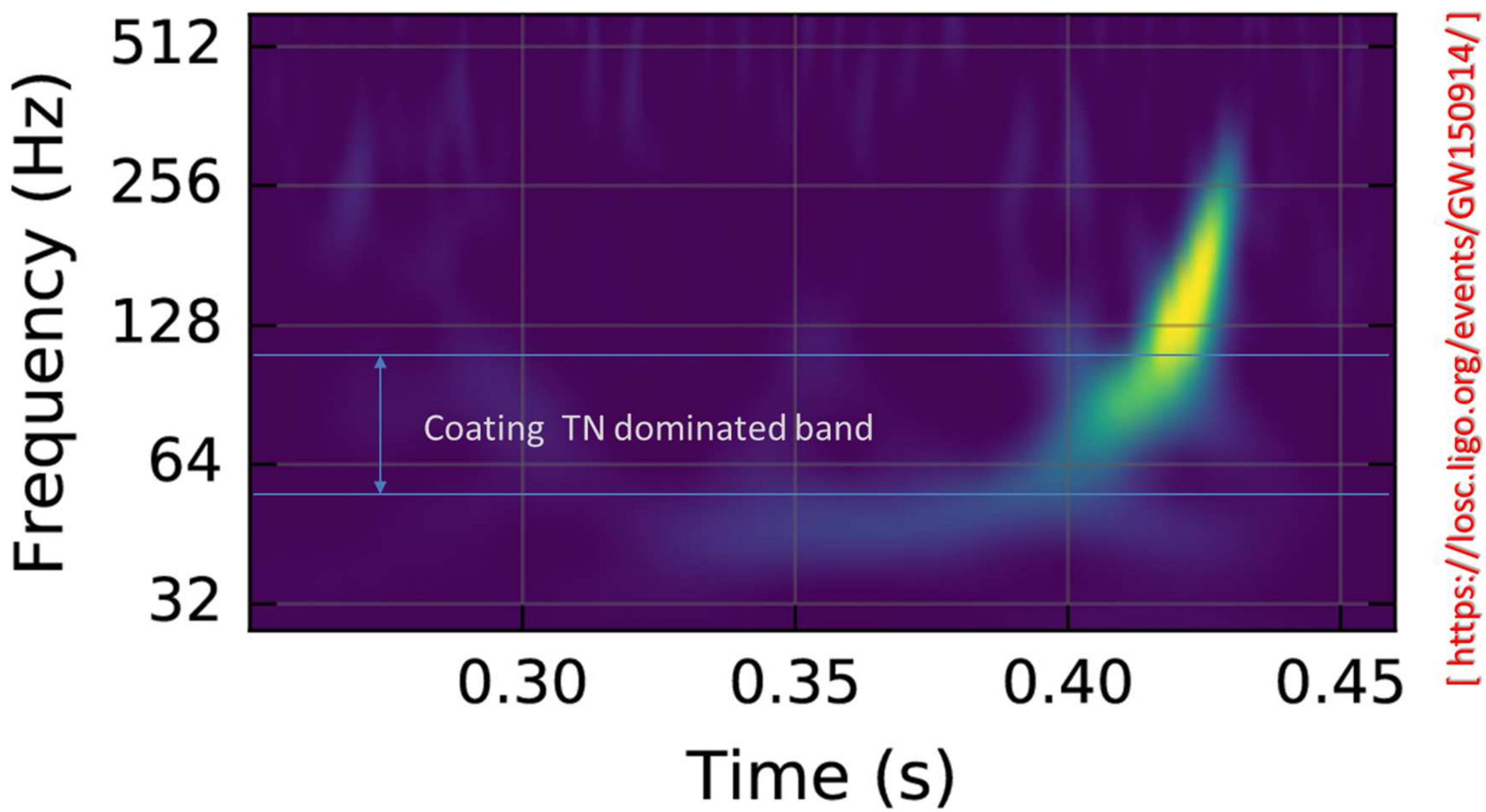

Coating R&D Funding

At the 1st "post detection" LVC Meeting in March 2016, the NSF re-presentatives solicited the LIGO coating working groups to submit a cooperative R&D on the subject, *worth 3M US$ on a 3y span*.

On July 7-8 2016 at the 2nd Dawn Workshop, hosted by Georgia Tech, a focus Session on coating R&D was held, where the proposal guidelines and the collaboration structure were set.

The final version of the proposal was completed on Dec. 16 2016.

There's no EGO-Virgo counterpart, as yet.

Coating R&D Funding in Italy

Coating R&D funding on behalf of Italian Research Agencies:

INFN COAT (Pinto et al.)
INFN MiDiBRUT (Pinto et al.)
MURST/MIUR COACH (Vetrano et al.)
INFN AdCOAT (Pinto et al.)

… worth *a few* tens KEUR total …

Outlook

Why Coating R&D

➡ Where are we now : the aLIGO mirrors

How can we progress:

- Improving Modeling
- Improving Processes
- Improving Characterization

Ongoing Studies & New Ideas:

- Nanolayered Composites
- Silicon Nitrides
- Crystalline Coatings
- M-ary Coatings
- Metamaterial Coatings

Conclusions

Basic Coating Noise Formula

Temperature

Coating loss angle (mechanical, F/D theorem)

$$S_{coat}^{(B)}(f) = \frac{2k_B T}{\sqrt{\pi^3} f} \frac{1-\sigma^2}{w_m Y} \phi_c$$

Beam spot-size

Act on the thicknesses

Act on the materials

$$\phi_c = \frac{\lambda_0}{w\sqrt{\pi}} \left(\eta_L d_L + \eta_H d_H \right), \quad \eta_{L,H} = \frac{\phi_{L,H}}{n_{L,H}} \left(\frac{Y_{L,H}}{Y_s} + \frac{Y_s}{Y_{L,H}} \right)$$

total *(H,L)*-index material thickness, in units of local wavelength

L,H material noisyness per unit thickness

LIGO Noise Floor Progress 2010-2015

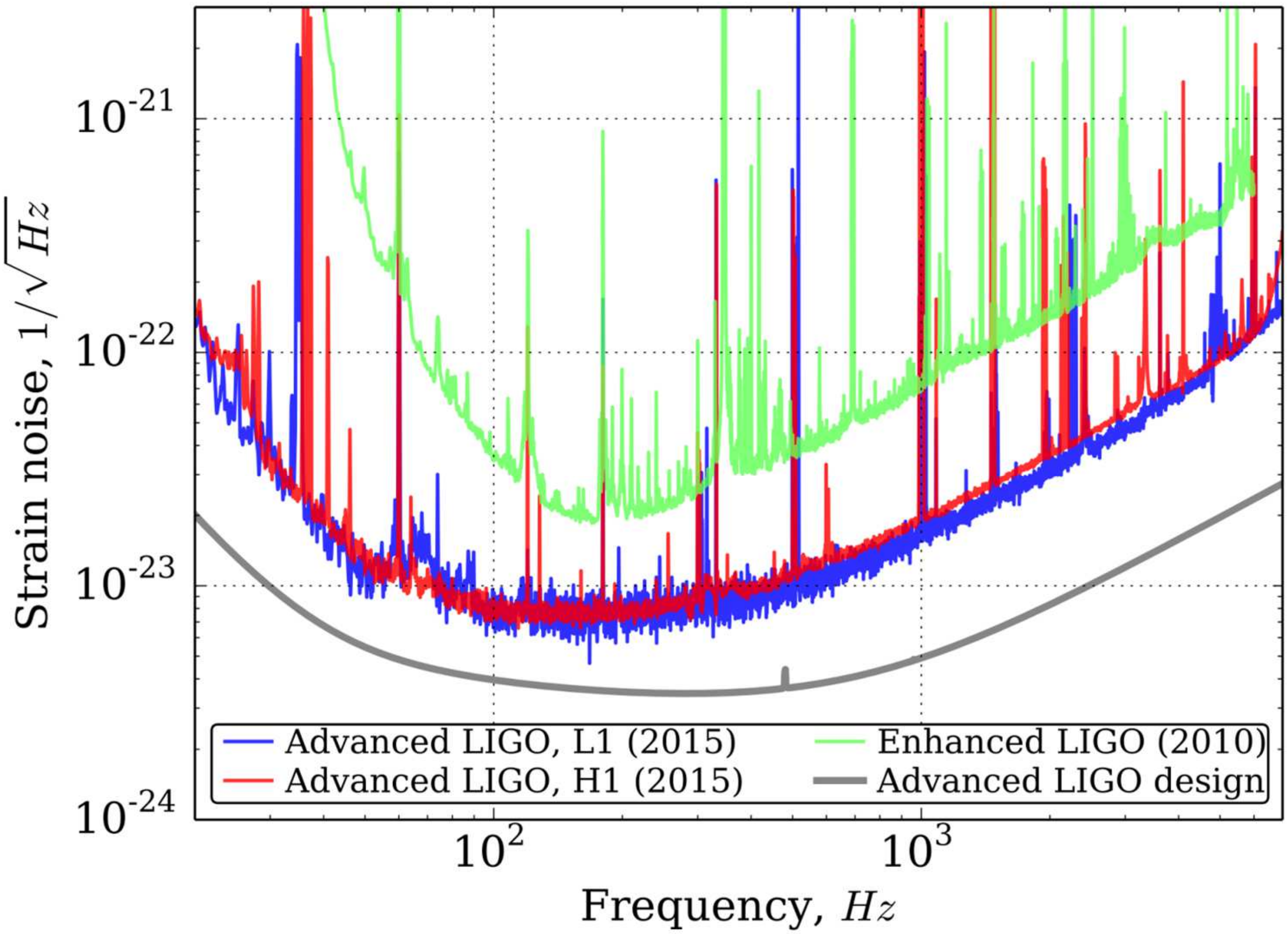

[Martynov et al., PRD 93 (2016) 112004]

The aLIGO Coatings

Major breakthrough # 1 : the development of Ti doped Tantala
[Harry et al, CQG 24 (2007) 405]

… Extensive trial and error testing (LMA, CSIRO) of alternative materials and dopants,

500nm thick films

	Refraction index	Absorption (ppm)	Mechanical losses
Ta_2O_5	2.035	1.22	$3{\cdot}10^{-4}$
Ta_2O_5 : Co	2.11	5000	$11{\cdot}10^{-4}$
Ta_2O_5 : W	2.07	2.45	$7.5{\cdot}10^{-4}$
Ta_2O_5 : W+Ti	2.06	1.65	$3.3{\cdot}10^{-4}$
➡ Ta_2O_5 : Ti	2.07	0.5	$2.4{\cdot}10^{-4}$

Coating	Refraction index	Absorption (ppm)	Mechanical losses
ZrO_2	2.10	11	$2.3{\cdot}10^{-4}$
ZrO_2 : Ti	2.15	37	$6.8{\cdot}10^{-4}$
ZrO_2 : W	2.12	10	$2.8{\cdot}10^{-4}$

[Flaminio et al., CQG 27 (2010) 84030] …

The aLIGO Coatings, contd.

Major breakthrough # 2 : coating thickness optimization

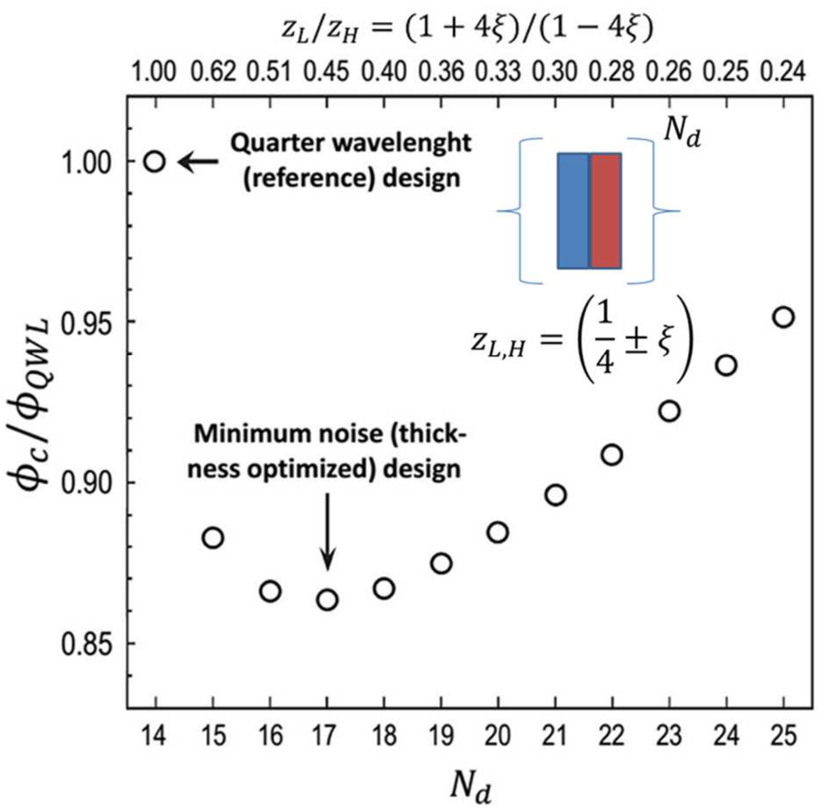

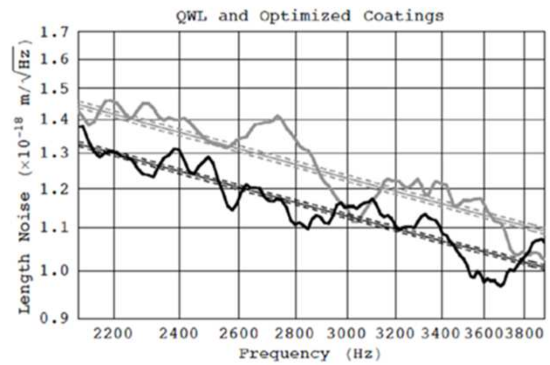

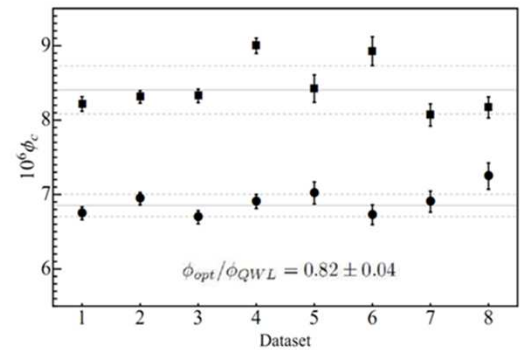

[Villar et al, PRD 81 (2010) 122001]

The aLIGO Coatings, contd.

…used for the aLIGO dichroic mirrors [Principe et al., LIGO T080337]

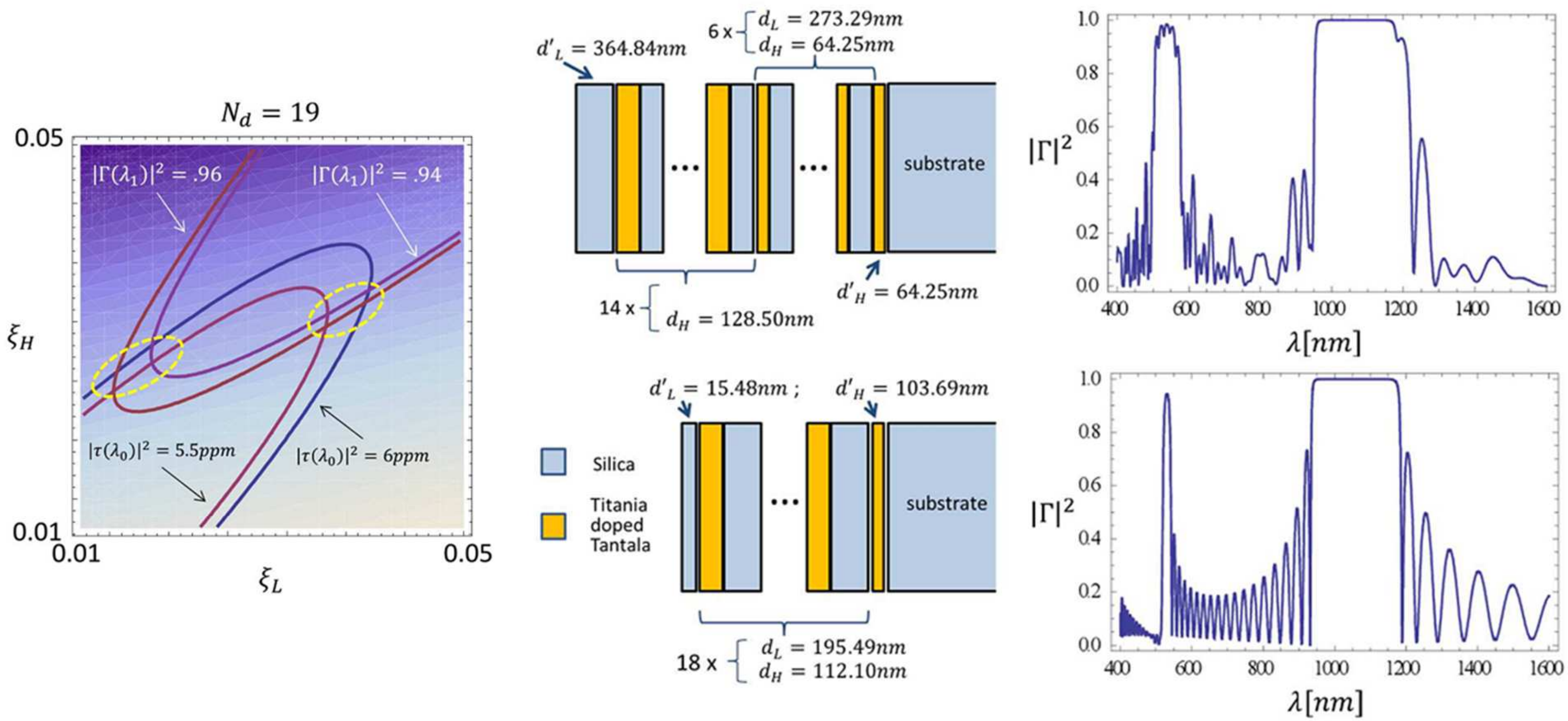

[Principe, Optics Expr 23 (2015) 10938]

Coating Science in "Milestone" Instrument Paper

PRL **116,** 131103 (2016) PHYSICAL REVIEW LETTERS week ending 1 APRIL 2016

GW150914: The Advanced LIGO Detectors in the Era of First Discoveries

B. P. Abbott *et al.*[*]
(LIGO Scientific Collaboration and Virgo Collaboration)
(Received 15 February 2016; published 31 March 2016)

Following a major upgrade, the two advanced detectors of the Laser Interferometer Gravitational-wave Observatory (LIGO) held their first observation run between September 2015 and January 2016. With a strain sensitivity of $10^{-23}/\sqrt{\mathrm{Hz}}$ at 100 Hz, the product of observable volume and measurement time exceeded that of all previous runs within the first 16 days of coincident observation. On September 14, 2015, the Advanced LIGO detectors observed a transient gravitational-wave signal determined to be the coalescence of two black holes [B. P. Abbott *et al.*, Phys. Rev. Lett. 116, 061102 (2016)], launching the era of gravitational-wave astronomy. The event, GW150914, was observed with a combined signal-to-noise ratio of 24 in coincidence by the two detectors. Here, we present the main features of the detectors that enabled this observation. At full sensitivity, the Advanced LIGO detectors are designed to deliver another factor of 3 improvement in the signal-to-noise ratio for binary black hole systems similar in mass to GW150914.

DOI: 10.1103/PhysRevLett.116.131103

Introduction.—On September 14, 2015, both Advanced LIGO detectors in the USA, H1 in Hanford, Washington and L1 in Livingston, Lousiana, made the first direct measurement of gravitational waves [1]. The event, GW150914, was determined to be the merger of two black holes, with masses of 36 and $29M_{\odot}$, into a black hole of approximately $62M_{\odot}$ [2]. 3.0 solar masses of energy ($\simeq 5.4 \times 10^{47}$ J) were radiated in gravitational waves. The gravitational waves from this event, which occurred at a distance of $\simeq 410$ Mpc $\simeq 1.3 \times 10^9$ light years, changed the separation between the test masses by $\simeq 4 \times 10^{-18}$ m, about one 200th of a proton radius.

The Advanced LIGO detectors, multikilometer Michelson-based interferometers [3], came online in September 2015, after a major upgrade targeting a factor of 10 sensitivity improvement over initial detectors [4,5]. While not yet at design sensitivity during their first observation run, they have already exceeded the strain sensitivity of the initial detectors across the entire frequency band, significantly surpassing the past discovery potential. This Letter describes the Advanced LIGO detectors, as well as their current and final design sensitivity, at the inception of gravitational-wave astronomy [6–10].

Astrophysical reach.—In general relativity, a gravitational wave far from the source can be approximated as a time-dependent perturbation of the space-time metric, expressed as a pair of dimensionless strain polarizations, h_+ and $h_\times$ [11]. An interferometric gravitational-wave detector acts as a transducer to convert these space-time perturbations into a measurable signal [12]. The interferometer mirrors act as "freely falling" test masses. Advanced LIGO measures linear differential displacement along the arms which is proportional to the gravitational-wave strain amplitude. We define the differential displacement as $\Delta L = \delta L_x - \delta L_y$, where $L_x = L_y = L$ are the lengths of two orthogonal interferometer arms. The gravitational-wave strain and the interferometer displacement are related through the simple equation $\Delta L = hL$, where h is a linear combination of h_+ and $h_\times$.

The tiny displacements induced by astrophysical events demand that the interferometer mirrors be free from environmental disturbances and require a highly sensitive interferometric transducer—designed to be limited only by disturbances arising from fundamental physics considerations. Since the interferometer response to displacement, or equivalently gravitational-wave strain, is frequency dependent, it is necessary to represent the limiting detector noises as functions of frequency normalized by the interferometer response.

The left panel of Fig. 1 shows the amplitude spectral density of the total strain noise in units of strain per $\sqrt{\mathrm{Hz}}$ during the first observation run (O1 run) and, for comparison, during the final science run of the initial LIGO detectors (S6 run). In the detectors' most sensitive frequency band between 100 and 300 Hz, the O1 strain noise is 3 to 4 times lower than that achieved in the S6 run. At 50 Hz, the improvement is about a factor of 30.

The right panel of Fig. 1 shows the single detector signal-to-noise ratio (SNR) for an optimally oriented compact binary system consisting of two $30M_{\odot}$ black holes as a function of redshift z and for different interferometer configurations. The observed strain amplitude is largest for a source whose orbital plane is parallel to the plane of the detector and is located straight above or below; we refer to such a source as optimally oriented. The SNR is computed in the frequency domain [14] using standard cosmology [15] and phenomenological waveforms which account for inspiral, merger, and ringdown, but not spins [16].

[*]Full author list given at the end of the article.

0031-9007/16/116(13)/131103(12) 131103-1

The mirror coatings, a dielectric multilayer of silica and titania-doped tantala [30,31], were developed to provide the required high reflectivity while minimizing coating thermal noise [32–34]

(p. 131103-3)

[29] G. Harry, T. P. Bodiya, and R. DeSalvo, *Optical Coatings and Thermal Noise in Precision Measurement* (Cambridge University Press, Cambridge, England, 2012).
[30] G. M. Harry *et al.*, Titania-doped tantala/silica coatings for gravitational-wave detection, Classical Quantum Gravity **24**, 405 (2007).
[32] R. Flaminio, J. Franc, C. Michel, N. Morgado, L. Pinard, and B. Sassolas, A study of coating mechanical and optical losses in view of reducing mirror thermal noise in gravitational wave detectors, Classical Quantum Gravity **27**, 084030 (2010).
[33] J. Agresti, G. Castaldi, R. DeSalvo, V. Galdi, V. Pierro, and I. M. Pinto, Optimized multilayer dielectric mirror coatings for gravitational wave interferometers, Proc. SPIE Int. Soc. Opt. Eng. **6286**, 628608 (2006).
[34] A. E. Villar *et al.*, Measurement of thermal noise in multilayer coatings with optimized layer thickness, Phys. Rev. D **81**, 122001 (2010).

(p. 131103-6)

the Australian Research Council. The authors gratefully acknowledge the Italian Istituto Nazionale di Fisica Nucleare (INFN), the French Centre National de la Recherche

(p. 131103-5)

* I. M. Pinto,[87] - [87]*University of Sannio at Benevento, I-82100 Benevento, Italy and INFN, Sezione di Napoli, I-80100 Napoli, Italy*

… Large Part of that Work was "Made in Italy"!

Optimized multilayer dielectric mirror coatings for gravitational wave interferometers

Juri Agresti[a,b], Giuseppe Castaldi[c], Riccardo DeSalvo[a], Vincenzo Galdi[c], Vincenzo Pierro[c], and Innocenzo M. Pinto[c]

[a] LIGO Laboratory, California Institute of Technology, Pasadena, CA 91125, USA;
[b] Department of Physics, University of Pisa, I-56127, Pisa, Italy;
[c] Waves Group, Department of Engineering, University of Sannio, I-82100, Benevento, Italy

ABSTRACT

The limit sensitivity of interferometric gravitational wave antennas is set by the thermal noise in the dielectric mirror coatings. These are currently made of alternating quarter-wavelength high/low index material layers with low mechanical losses. The quarter-wavelength design yields the maximum reflectivity for a fixed number of layers, but *not* the lowest noise for a prescribed reflectivity. This motivated our recent investigation of *optimal* thickness configurations, which guarantee the lowest thermal noise for a targeted reflectivity. This communication provides a compact overview of our results, involving *nonperiodic genetically-engineered* and *truncated periodically-layered* configurations. Possible implications for the advanced Laser Interferometer Gravitational wave Observatory (LIGO) are discussed.

Advances in Thin-Film Coatings for Optical Applications III, edited by Michael J. Ellison,
Proc. of SPIE Vol. 6286, 628608, (2006) · 0277-786X/06/$15 · doi: 10.1117/12.678977

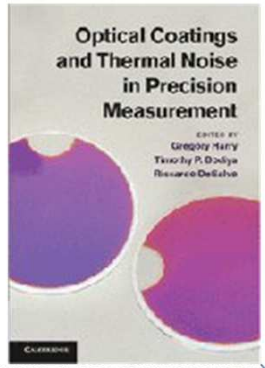

ISBN: 9781107003385 (2012)

12

Reflectivity and thickness optimization

INNOCENZO M. PINTO, MARIA PRINCIPE, AND RICCARDO DESALVO

12.1 Introduction

This chapter is focused on design strategies for minimizing Brownian (see Chapter 4) and, more generally, thermal noises (see Chapters 3 and 9) in high-reflectivity optical coatings. It is organized as follows: in Section 12.2 we review the basic formulas needed to describe the optical properties of dielectric coatings (an *ab-initio* derivation of these formulas is included in the Appendix). Brownian noise formulas are the subject of Section 12.3. Section 12.4 presents the key ideas of coating thickness optimization. Thermo-optic noise issues are reviewed in Section 12.5, together with a discussion of pertinent minimization criteria. Section 12.6 contains a few comments on material characterization, and touches the important topic of glassy mixture modeling and optimization.

12.2 Coating formulas

In this section we summarize the basic coating formulas on which the subsequent analysis is based. A compact *ab-initio* derivation of these results is given in the Appendix.

Optical coatings are modeled as stacks of planar layers terminated on both sides by homogeneous halfspaces; the relevant geometry and notation is sketched in Figure 12.1. Layers are identified by an index $i = 1, 2, \ldots, N_L$. It is understood that $i = 0$ and $i = N_L + 1$ correspond to the left halfspace and the substrate, respectively. It is convenient to introduce a local coordinate system (x, y, z_i) for each layer, so that the internal layers $i = 1, 2, \ldots, N_L$ correspond to $-d_i \leq z_i \leq 0$, the left halfspace is defined by $-\infty < z_0 \leq 0$, and the substrate by $0 \leq z_{N_L+1} < \infty$. Plane wave incidence from the leftmost halfspace is assumed.[1] An $\exp(\imath 2\pi f t)$ time dependence of the field is understood and omitted.

[1] This is the usual (optical limit) approximation. The general case of an incident Gaussian beam, and its optical limit, are discussed in Hillion (1994).

Optical Coatings and Thermal Noise in Precision Measurement, eds. Gregory M. Harry, Timothy Bodiya and Riccardo DeSalvo. Published by Cambridge University Press. © Cambridge University Press 2012.

PHYSICAL REVIEW D **81**, 122001 (2010)

Measurement of thermal noise in multilayer coatings with optimized layer thickness

Akira E. Villar, Eric D. Black, Riccardo DeSalvo, and Kenneth G. Libbrecht
LIGO Laboratory, California Institute of Technology, Mail Code 264-33, Pasadena, California 91125, USA

Christophe Michel, Nazario Morgado, and Laurent Pinard
Laboratoire des Matériaux Avancés, Université Claude Bernard Lyon 1, CNRS/IN2P3, Villeurbaune, France

Innocenzo M. Pinto, Vincenzo Pierro, Vincenzo Galdi, Maria Principe, and Ilaria Taurasi
Waves Group, University of Sannio at Benevento, Benevento, Italy, INFN and LSC
(Received 7 April 2010; published 3 June 2010)

A standard quarter-wavelength multilayer optical coating will produce the highest reflectivity for a given number of coating layers, but in general it will not yield the lowest thermal noise for a prescribed reflectivity. Coatings with the layer thicknesses optimized to minimize thermal noise could be useful in future generation interferometric gravitational wave detectors where coating thermal noise is expected to limit the sensitivity of the instrument. We present the results of direct measurements of the thermal noise of a standard quarter-wavelength coating and a low noise optimized coating. The measurements indicate a reduction in thermal noise in line with modeling predictions.

DOI: 10.1103/PhysRevD.81.122001

Innocenzo M. Pinto - ICORE

Rome, IT, March 2, 2016

Centro Fermi
Museo Storico della Fisica e
Centro Studi e Ricerche Enrico Fermi

The Advanced LIGO Mirrors

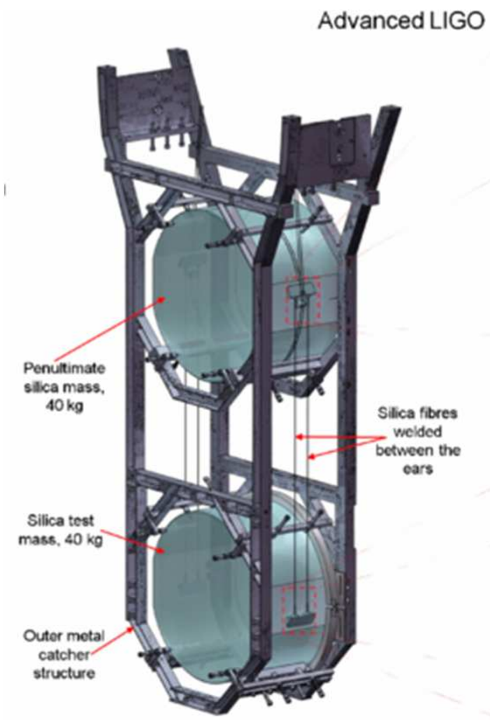

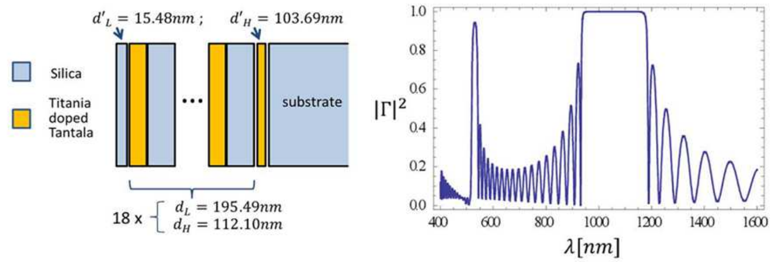

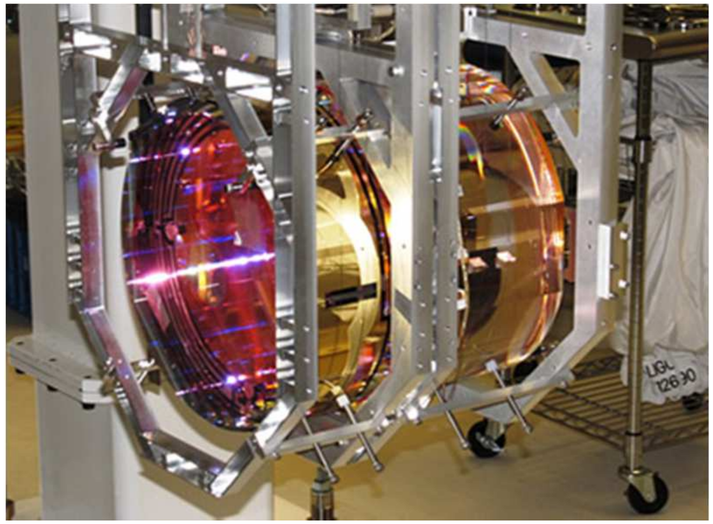

Designed by the Usannio LSC Working Group, manufactured by LMA (Lyon, FR)

Outlook

Why Coating R&D

Where are we now : the aLIGO mirrors

How can we progress:

- Improving Modeling
- Improving Processes
- Improving Characterization

Ongoing Studies & New Ideas:

- Nanolayered Composites
- Silicon Nitrides
- Crystalline Coatings
- M-ary Coatings
- Metamaterial Coatings

Conclusions

Atomic Level Investigations

- Experimental techniques that aim to link macroscopic material properties to the coating atomic structures:

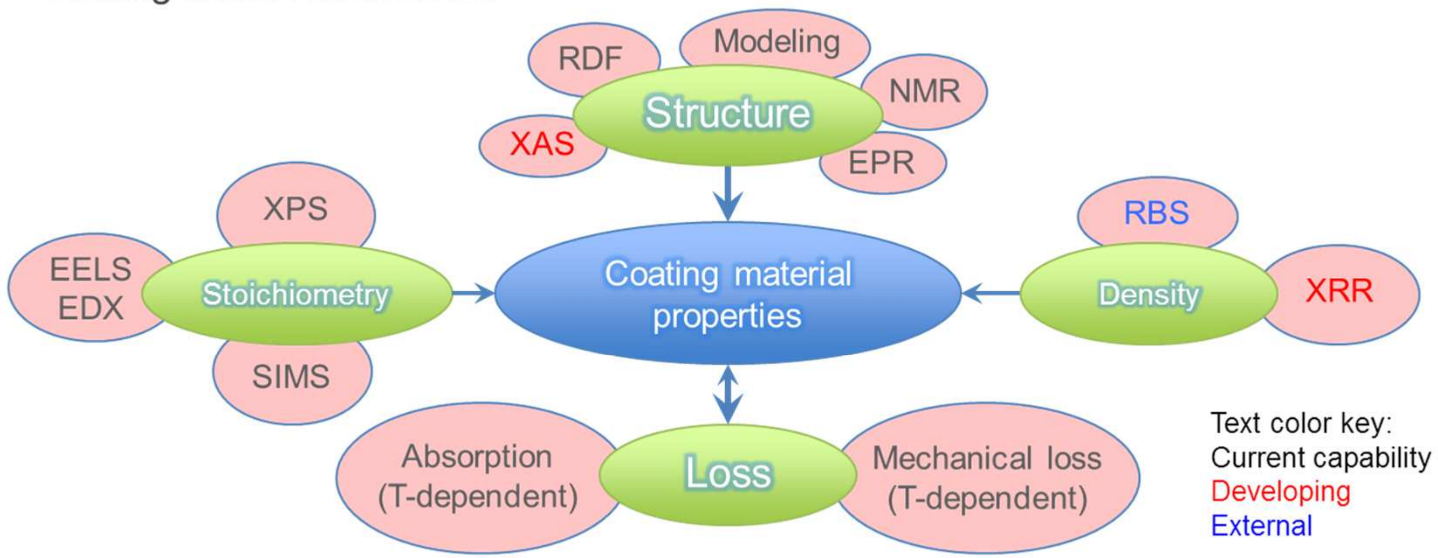

- RDF – Reduced Density Function
- NMR – Nuclear Magnetic Resonance
- XAS – X-ray Absorption Spectroscopy
- XPS – X-ray Photoelectron Spectroscopy
- EPR – Electron Paramagnetic Resonance
- RBS – Rutherford Backscattering Spectrometry
- EELS – Electron Energy Loss Spectroscopy
- EDX – Energy Dispersive X-ray (Spectroscopy)
- XRR – X-ray Reflectometry
- SIMS – Secondary Ion Mass Spectrometry

Working groups : Stanford, Glasgow

[Bassiri et al., LIGO-G100620]

TLS Model

Acoustic (sound velocity & attenuation), dielectric (light velocity & attenuation) and thermal (specific heat & thermal conductivity) properties of amorphous solids display *generic features*, consistent with a model where local clusters of a few atoms/molecules may switch between two different configurations, as an effect of thermal or quantum fluctuations. Transitions produce dissipation, and hence noise.

The above two-level systems (TLS) are described (in suitable configuration coordinates) by double-well potentials, uniquely identified by the distributions of the barrier height *V*, unbalance Δ, and switch time τ.

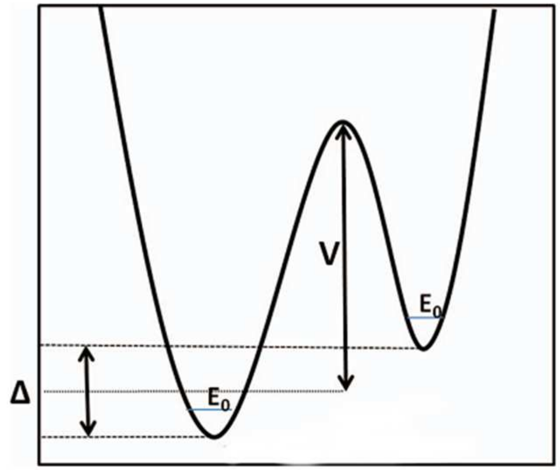

[Gilroy & Phillips, Phil. Mag. B38 (1981) 735]

TLS Model, contd.

Mechanical losses (and other properties) can be derived from knowledge of those distributions via simple formulas [Pohl et al., Rev. Mod. Phyis. 74 (2002) 991; Gilroy & Phillips, Phil. Mag. B38 (1981) 735].

Both phonons and photons can drive TLS transitions. Measurements show that acoustic attenuation (mechanical loss) is reduced upon simultaneous RF exposure. [Laermans et al. J. Phys. C: Solid State Phys. 10 (1977) L161]. This is possibly interesting. (Brought to the attention of this Community by M. Abernathy)

The TLS model is corroborated by brute force molecular modeling [Hamdan et al., J. Chem. Phys. 141 (2014) 054501; Trinastic et al., Phys. Rev. B 93 (2016) 014105],

Molecular Dynamics

Investigates mechanical loss in amorphous oxides using classical MD software (e.g., DL-POLY) to calculate barrier height and asym-metry distributions, relaxation times, and deformation potentials.

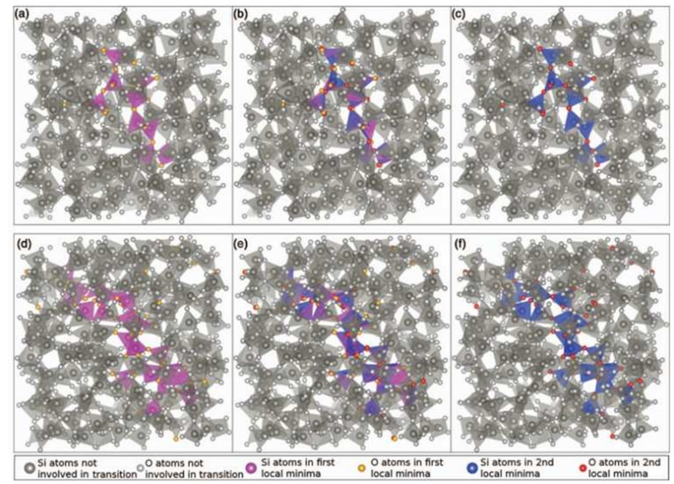

Silica - the top (panels (a)–(c)) involve 21 atoms; the bottom ones ((d)–(f)) 59. Atoms in gray are not involved in the transitions

Results match experimental trends Showing that that titania doping decreases the magnitude of the low-temperature loss peak in Tantala.

May eventually help optimizing glassy oxide mixture formulations.

Working groups : UFL Gainsville

Outlook

Why Coating R&D

Where are we now : the aLIGO mirrors

How can we progress:

- Improving Modeling
- Improving Processes
- Improving Characterization

Ongoing Studies & New Ideas:

- Nanolayered Composites
- Silicon Nitrides
- Crystalline Coatings
- M-ary Coatings
- Metamaterial Coatings

Conclusions

Better Depositions

- Films created by "hot" deposition ($T \lesssim T_g$) featuring *negligible bulk mobility* but *large surface mobility* yield nearly ***ideal glasses*** with ***almost no TLS*** (thought of as due to energy landscape sampling by the depositing molecules).

- Such behavior is ***observed in quite different materials***, e.g. *Indomethacin* [T. Perez et al., PNAS 111 (2014) 11275] and *a-Silicon* [X. Liu et al., Phys. Rev. Lett. 113 (2014) 025503], and is **credited as *generic*** [Ediger, PNAS 111 (2014) 11232]

➡ E-beam hot ($T \sim 0.8\, T_g$) deposited *a*-Si films display TLS densities and elastic losses a factor 100 lower than conventional (LT deposited & HT annealed) films [X. Liu et al, ibid.]

Better Depositions, contd.

- … a pratical way [Kearns et al., J. Phys. Chem. B112 (2008) 4934] to check the (paradoxical/controversial) Kauzmann ansatz [Kauzmann, Chem. Rev. 43 (1948) 219]

- **… yet to be proved for the glassy oxides of our interest …**

- … requires deposition tools enabling *high surface mobility* (high surface temperature) and *low deposition rates* [Singh et al., Nature Mat. 12 (2013) 139; ibid 13 (2014) 662; Lyubimov et al. J. Chem. Phys. 139 (2013) 144505]

- **The required deposition temperature may be too high for the needed large(st) IBS systems**

- **Enhanced mobility may boost crystallite formation → scattering**

Smarter Doping

Crystallization frustration following thermal annealing can be achieved also by doping.

Silica doping prevents Hafnia from crystallizing [Ushakov et al. Ph. Stat. Sol. B241 (2004) 2800]; Zirconia doping prevents Tantala from crystallizing [Penn LIGO-G1301031]; Silica prevents Zirconia from crystallizing [Penn, LIGO-G1300306], etc.

Doping may have different effects: Titania affects strongly Oxygen-Tantalum coordination, reducing mechanical losses in Ta2O5; Hydrogen doping reduces mechanial losses in *a*-Si, etc.

One may use *different dopants together*, to obtain different effects…
… or use *(nano)-stratified* mixtures

Nanolayered vs Cosputtered

[I. Pinto, LIGO-G1100586]

SiO_2/TiO_2 Composites

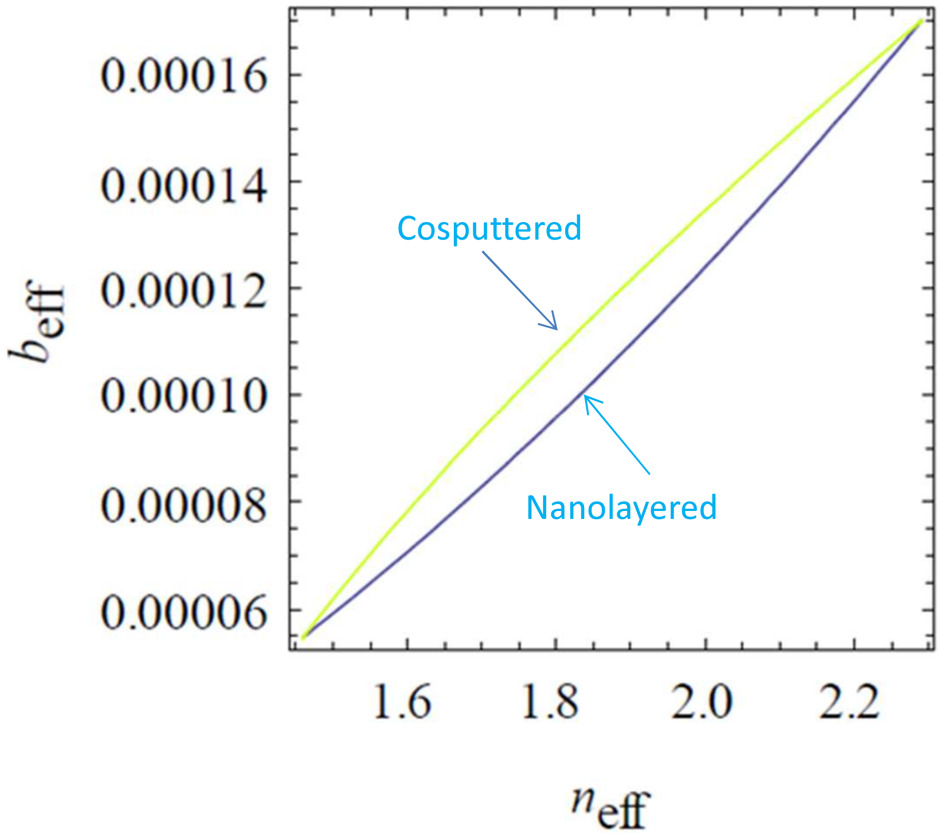

Nanolayered SiO2/TiO2 composites are *less noisy* , compared to co-sputtered SiO2/TiO2 composites having *the same refraction index*

University-Scale Coating Facilities

... involved in GW detector collaborations **(as of Jan 2017)**

- **UCB**, Berkeley CA, USA (PI Frances Hellman)
  EB, RF-MS, PDC-R-MS
- **CSU**, Fort Collins CO, USA (PI Carmen Menoni)
  (D)IBS
- **NAOJ/ATC**, Tokyo, JP (PI Waseda Kouichi)
  IBS
- **NTHU**, Taipei, TW (PI Shiuh Chao)
  IBS, CVD
- **UWS**, Paisley, UK (PI Stuart Reed)
  PA-EB, MA-RS, PE-CVD, IA-RFS
- **USANNIO**, Benevento, IT (PI Maria Principe)
  PA(D)EB

University-Scale Coating Facilities, contd.

Abbreviations:

- *EB = Electron Beam Gun Evaporator*
- *RF-MS =Radio Frequency Microwave Sputtering*
- *PDC-R-MS =Pulsed DC Reactive Magnetron Sputtering*
- *(D)IBS = (Dual) Ion Beam Sputtering*
- *PA-EB = Plasma Assisted EB*
- *MA-RS = Microwave assisted Reactive Sputtering,*
- *PE-CVD =Plasma Enhanced Chemical Vapor Deposition*
- *IA-RFS – Ion Assisted Radio Frequency Sputtering*
- *PA(D)EB = Plasma Assisted (Dual) EB*

The USannio Coating Facility

Custom version of Optotech OAC-75

- Plasma assisted deposition
- High quality /density of layers
- Dual eb-gun
- Multimaterial
- Fully programmable
- Substrate heating
- R&D configuration
- IBS as possible add-on

Cost $\sim 0.6\ MEUR$

Funding by Regione Campania (FESR, University research empowering program)

Should start operatation in spring 2017

The USannio Coating Facility, contd.

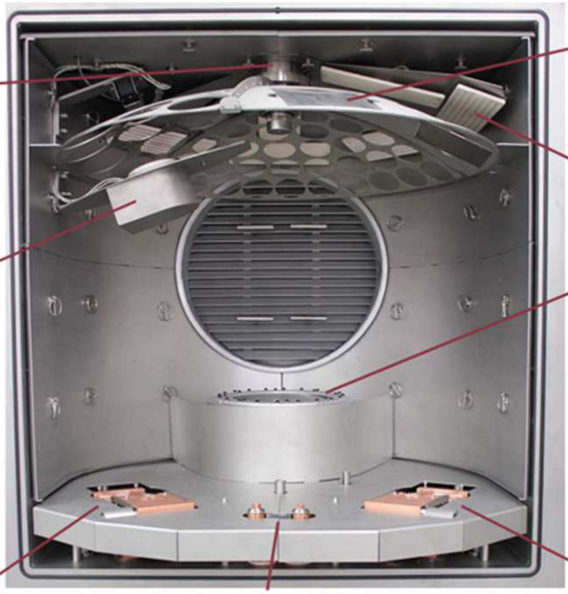

[Ferrotec EVM-8 eb-gun systems]

- 2 eb-guns
- Multiple (6) pocket configuration
- Evaporation of all kind of oxides (and metals)
- Co-evaporation of different optical materials possible
- Freely adjustable HV from 6 to 8 kV (layer-to-layer)
- Sweep parameters and sweep pattern easy preset
- Variable pocket rotation speed (single pocket)

(COPRA® IS200 plasma source)

- Built-in source w. flexible position & changeable inclination
- Powered @ 13.56 MHz, max. power 1500 W
- Large beam extraction Ø 110 mm for uniform distribution
- Ion energy 50 to 180 eV
- Ion current density up to 0.5 mA/cm²
- Pressure range 1E-4 to 1E-3 mbar
- Operation with pure oxygen possible
- Highest n-values for stress free films

Built in GUI-based MacroTech control unit
bles fully automated process control

The USannio Coating Facility, contd.

UniSa Nanotechnology Lab Facilities (F. Bobba, C. Di Giorgio)

- X-Ray Diffractometer X'PERT MRD-PRO (Philips)
- UHV-variable temperature AFM/STM (Omicron)
- Room temperature AFM/AFS MM5 (Bruker Nanowizard3 JPK)
- SEM EVO50 (Zeiss) ; FeSEM Σigma GEMINI (Zeiss) ; TEM TMG2 (Fei)

UHV-Cryo AFM/STM

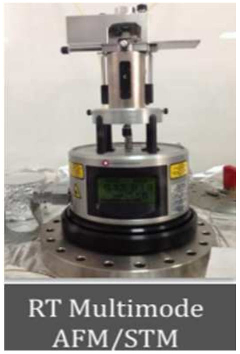

RT Multimode AFM/STM

Scanning Electron Microscope

Outlook

Why Coating R&D

Where are we now : the aLIGO mirrors

How can we progress:

- Improving Modeling
- Improving Processes
- Improving Characterization

Ongoing Studies & New Ideas:

- Nanolayered Composites
- Silicon Nitrides
- Crystalline Coatings
- M-ary Coatings
- Metamaterial Coatings

Conclusions

Direct TN Measurement : TNI etc.

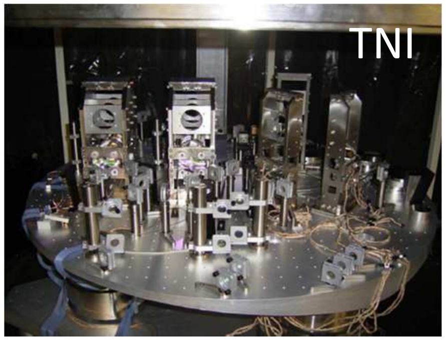

Original TNI
[Numata et al., Phys. Rev. Lett. 91 (2003) 260602]
[Black et al., Phys. Lett. A 328 (2004) 1]

Available facilities

- LMA (QDI) [Paolino et al., Rev. Sci. Instrum. 84, 2013]
- Caltech (TNI) [Chalermsongsak et al., Metrologia 52 (2015) 17]
- MIT (CTN) [Gras et al., Phys. Rev. D95, 022001 (2017)]

Other facilities (under development)

- AEI (10m facility), [Wohler et al. LIGO-P1600260]
- UFL, (Cryo-Thor) [Mueller et al., LIGO-G1600076]

Mechanical Loss from Ringdown : the Cantilever

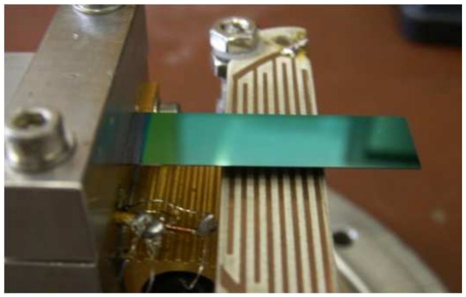

$$Q_c^{-1} = Q^{-1} + \frac{<W_s>}{<W_c>}\left(Q^{-1} - Q_s^{-1}\right)$$

$$\frac{<W_c>}{<W_s>} = \frac{\int_{h_s}^{h_s+h_c} (z-z_0)^2 \frac{E(z)}{\left(1-\sigma(z)^2\right)} dz}{\int_0^{h_s} (z-z_0)^2 \frac{E(z)}{\left(1-\sigma(z)^2\right)} dz} \approx \frac{E_s h_s}{3 E_c h_c}$$

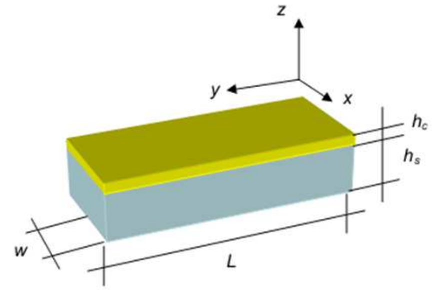

Fig. 1 – Problem's geometry and notation

LIGO –T060173

LIGO

LIGO Laboratory / LIGO Scientific Collaboration

LIGO-T060173-00-R | *LIGO* | Date August 3 2006

Measuring Coating Mechanical Quality Factors in a Layered Cantilever Geometry: a Fully Analytic Model

Vincenzo Pierro, Innocenzo M. Pinto

TWG, University of Sannio at Benevento, ITA

Distribution of this document:
LIGO Science Collaboration

This is an internal working note of the LIGO Project.

Reduction of tantala mechanical losses in Ta_2O_5/SiO_2 coatings for the next generation of VIRGO and LIGO interferometric gravitational waves detectors

Christophe Comtet [a,*], Danièle Forest [a], Patrick Ganau [a], Gregory M Harry [b], Jean Marie Mackowski [a], Christophe Michel [a], Jean Luc Montorio [a], Nazario Morgado [a], Vincenzo Pierro [c], Laurent Pinard [a], Innocenzo Pinto [c] and Alban Remillieux [a]

[a] *Laboratoire des Matériaux avancés, CNRS, France*
[b] *LIGO Laboratory, Massachusetts Institute of Technology, NW17-161, Cambridge, MA 01239, USA*
[c] *Waves Group, Department of Engineering, University of Sannio, I-82100, Benevento, Italy*

Abstract

Mirror thermal noise in Ta_2O_5/SiO_2 coatings is predicted to be the limiting noise in the 50-300 Hz frequency range in the interferometric gravitational wave detectors. Ta_2O_5 losses were dominating compared to the SiO_2 losses. We developed a model to calculate multilayer mechanical losses and we are working for low mechanical losses Ta_2O_5/SiO_2 coatings.

Keywords: Gravitational waves; thermal noise; mechanical losses

[in 42th Rencontres de Moriond : Gravitational Waves and Experimental Gravity, 2007]

Mechanical Loss from Ringdown : GeNS

The Gentle nodal Suspension (GeNS) is to date the most reliable mechanical loss estimation setup based on ringdown measurement.

Several improvements compared to clamped cantilever systems;

Designed to be exempt from re-clamping issues, yields nicely repeatable results.

Multimode operation should allow measurement of bulk/shear loss angles (TBD).

Available facilities:

- **LMA (G. Cagnoli)**
- **Rome-TV (E. Cesarini)**
- **Caltech (G. Vajente)**

[Cesarini et al., Rev. Sci. Instrum. 80 (2009) 053904.]

Cryogenic Loss Measurements

- Are needed for downselection of coating materials to be used in 3rd generation (cryogenic) GW detectors;

- Can be used to retrieve the activation energy and relaxation time distributions of a TLS model, **from the frequency dependence of the loss peak temperature** by plotting $\log[f]$ vs T, so as to obtain (E_a, τ), in view of

$$2\pi f \tau \exp[E_a/kT] = 1$$

- Help understanding how deposition & annealing affect losses.

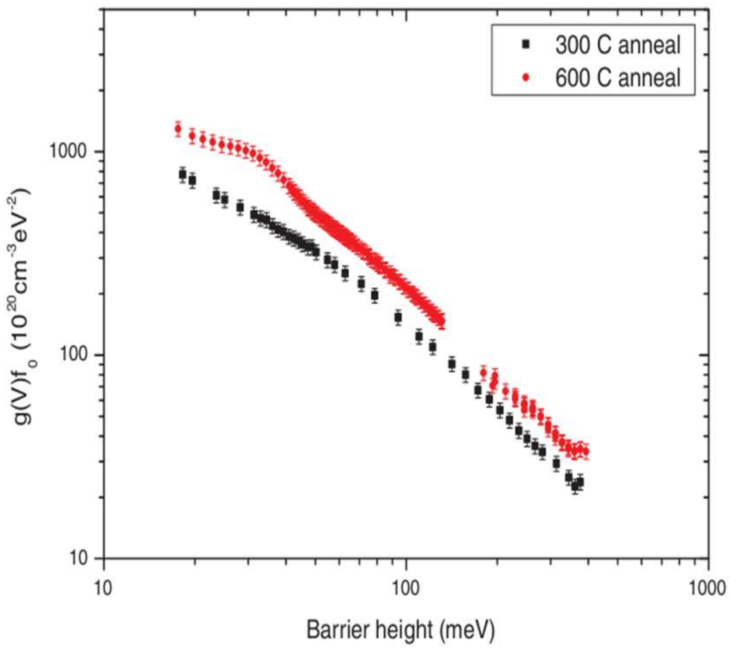

Available facilities : several, e.g.

Glasgow, LMA, NTHU , Perugia, Rome, Stanford, etc.

[Martin et al., CQG 27 (2010) 225020]

Measuring Elastic Moduli (Y,σ)

Several techniques proposed : acoustic (ERAU), nano-indentation (Glasgow) , resonance-shift (USannio), partly complementing. Working facilities at

- **ERAU [A. Gretarsson (a)]**
- **Glasgow [I. Martin (n)]**
- **Caltech [M. Abernathy (n)]**
- **LMA [G. Cagnoli (n)]**

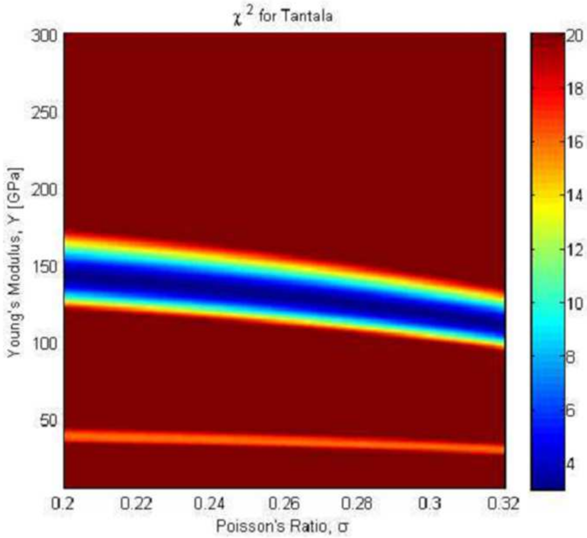

Not only an ingredient of the coat-TN formula, but also needed to compute the *dilution factors* relating material loss angles to measured ringdown damping times.

[Rhoades et al., LIGO-T1500147]
[Abernathy et al., Appl. 53 (2014) 3196]

Direct (TNI) vs Ringdown

Material	Layer thickness (nm)	ϕ ($\times 10^{-4}$)	Setup/ref
SiO_2	90.8–272.3	0.5 ± 0.3	Suspended disks [12]
	181.5–250.984	0.51 ± 0.07	TNI
	500	0.5 ± 0.018	Clamped cantilevers [27]
	500	0.46 ± 0.01	Clamped cantilevers [28]
	3,070	0.6 ± 0.03	Quad. Phase Diff. IFO [29]
Ta_2O_5	65.36–196.07	4.4 ± 0.2	Suspended disks [12]
	80.688–130.713	4.72 ± 0.14	TNI
	133	3.3 ± 0.9	GeNS [30]
	500	3.02 ± 0.11	Clamped cantilevers [27]
	3,130	4.7 ± 0.2	Quad. Phase Diff. IFO [29]
$TiO_2:Ta_2O_5$	112.10–128.8	3.66 ± 0.26	TNI
	500	2.4 ± 0.4	Clamped cantilevers [28]

References

[12] S. D. Penn et al., CQG 20 (2003) 2917
[27] Ch. Comtet et al., Proc. 42th Renc. Moriond (2007) http://hal.in2p3.fr/docs/00/17/75/78/PDF/Conf3.pdf
[28] R. Flaminio et al., Proc. GWADW 2013 (Elba) https://agenda.infn.it/getFile.py/access?contribId=105&sessionId=26&resId=0&materialId=slides&confId=5484
[29] M. Granata et al., Proc. GWADW 2014 (Takayama) http://www.gravity.ircs.titech.ac.jp/GWADW2014/slide/Massimo_Granata.pdf
[30] E. Cesarini et al., J. Non-Cryst. Solids 357 (2011) 2005
[41] R. Flaminio et al., Proc. 9th Amaldi Conference, http://www.amaldi9.org/abstracts/420/Flaminio_Amaldi_2011_July11.pdf

Direct (TNI-derived) loss angle estimates [Principe et al, Phys Rev. D-91 (2015) 022 005] **are in good agreement with available (LMA) quad-phase differential interferometry results (Silica and Plain Tantala).**

[Principe et al., PRD 91 (2015) 022005]

More Loss Measurement Puzzles

Puzzle # 1 (multilayers)

Use (measured) loss angle of multilayer, and (measured) loss angle of single low (resp. high) index material to estimate loss angle of high (resp. low) index mateial. Results are inconsistent :

$\phi_{H^*} = (2.4 \pm 0.2) \cdot 10^{-4} \Longrightarrow \phi_L = (1.3 \pm 0.4) \cdot 10^{-4}$

$\phi_L = (0.5 \pm 0.1) \cdot 10^{-4} \Longrightarrow \phi_{H^*} = (4.2 \pm 0.2) \cdot 10^{-4}$

Puzzle # 2 (multilayers)

Double-face vs single face coating :

1) suppresses (post annealing) substrate bending.

2) total loss should be doubled, i.e., $Q_2 = Q_1/2$

Measurements : confirm this for single-layer films;.

instead, for multi-layers, one gets $Q_2 > Q_1/2$.

does bending suppression alleviate interface friction ?

More Loss Measurement Puzzles

Mechanical loss measurements on multi-layer Titania-doped-Tantala/Silica coatings on Silicon (annealed at 400 C~ 600 C) show a cryo-peak at ~ 30K **[Granata et al., Opt. Lett. 38, 5268 (2013)].**

Mechanical loss measurements on multi-layer Tantala/Silica coatings on Sapphire do *not* show such peak, yielding almost temperature-independent losses **[Yamamoto et al., PRD-74 022002 (2006); Hirose et al., LIGO-P1400107]** .

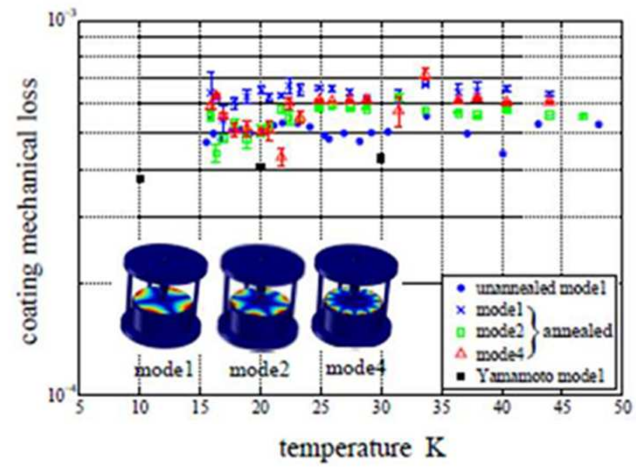

Reasons behind these discrepancies yet to be understood .

Issues with $\phi_{\parallel}$, $\phi_{\perp}$

1) "Traditional" definition of coating loss angle [Harry et al., CQG **29** (2002) 897]

$$\frac{\phi_c}{d} = \left(\frac{\delta U_{\parallel}}{U}\right)\phi_{\parallel} + \left(\frac{\delta U_{\parallel}}{U}\right)\phi_{\perp}, \text{ where}$$

$$\delta U_{\parallel} = \int_s \frac{1}{2}(S_{xx}T_{xx} + S_{yy}T_{yy})\,dxdy$$

$$\delta U_{\perp} = \int_s \frac{1}{2} S_{zz}T_{zz}\,dxdy$$

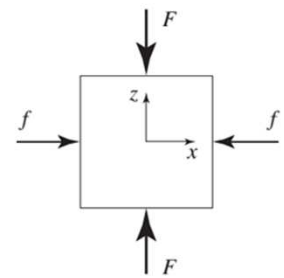

is **ill defined**, as the "Energies" $\delta U_{\parallel}$, $\delta U_{\perp}$ can be negative in some cases (e.g. symmetrically squeezed cube).

[Hong, PhD Thesis., Caltech 2013]

2) "Traditional" definition of $\phi_{\parallel}$, $\phi_{\perp}$ [Harry et al., CQG **29** (2002) 897]

$$\phi_{\perp} = Y_{\perp}\left(\frac{Y_1^{-1}\phi_1 d_1 + Y_2^{-1}\phi_2 d_2}{d_1 + d_2}\right), \quad \phi_{\parallel} = Y_{\parallel}^{-1}\left(\frac{Y_1\phi_1 d_1 + Y_2\phi_2 d_2}{d_1 + d_2}\right)$$

Holds, strictly, **only** for $\sigma_1 = \sigma_2 = 0$ (which implies $\phi_B = \phi_S$) .

[Somiya, LIGO T0900033v1]

…Use Bulk & Shear Loss Angles

Write elastic energy in terms of bulk and shear deformations/stresses

$$U = \frac{1}{2}K\Theta^2 + \mu\Sigma_{ij}\Sigma_{ij}$$

bulk / shear energies

where $\begin{cases} \Theta = S_{ii} \text{ , } S = \text{stress tensor} \\ \Sigma = \frac{1}{2}(S_{ij}+S_{ji}) - \frac{1}{3}g_{ij}S_{kk} \end{cases}$

Express coating loss angle in terms of bulk/shear loss angles

$$\frac{\phi_C}{d} = \left(\frac{\delta U_B}{U}\right)\phi_B + \left(\frac{\delta U_S}{U}\right)\phi_S$$

bulk/shear dilution factors

Calculate dilution factors using FEA .
Requires accurate knowledge of coating (bulk) Young and Poisson moduli.

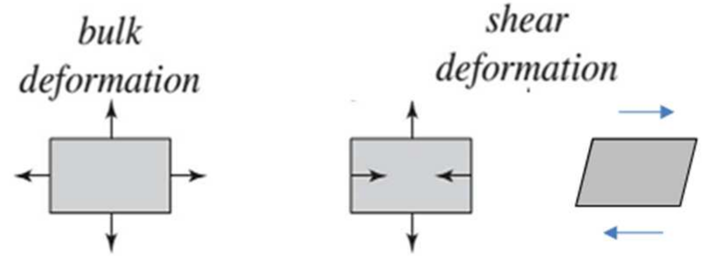

1) Bending (Transverse) Modes of Coated Thin Rectangular Plate

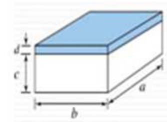

$$\phi = \frac{d}{c}\frac{Y_c}{Y_s}\frac{(1-\sigma_s^2)}{(1-\sigma_c)^2}\left[\phi_B(1-2\sigma_c) + 2\phi_s\frac{1-\sigma_c+\sigma_c^2}{1+\sigma_c}\right] + \phi_{sub}$$

2) Torsional Modes of Coated Thin Hollow Cylinder
[L. H. Donnell, NACA Rept 479, (1933)]

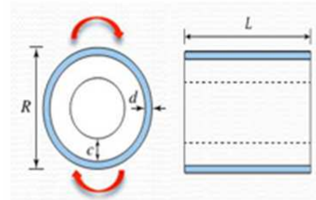

$$\phi = \phi_{sub} + \frac{d}{c}\frac{Y_c}{Y_s}\frac{(1+\sigma_s)}{(1+\sigma_c)}\phi_S$$

[T. Hong, PhD Thesis, Caltech, 2013]

[Harry, LIGO-G1500109]

Bulk & Shear Loss Angle Measurement

… from measured ringdown of several butterfly (b) and drumhead (d) modes via

measured   dil. factor matrix (FEA, known)   sought

$$\begin{pmatrix} \phi_b \\ \phi_d \\ \dots \end{pmatrix} = \begin{pmatrix} R_{bulk-b} & R_{shear-b} \\ R_{bulk-d} & R_{dhear-d} \\ & \dots \end{pmatrix} \begin{pmatrix} \phi_B \\ \phi_S \\ \dots \end{pmatrix}$$

[Abernathy, LIGO-G1300163
Harry et al., LIGO-G1400803
Harry et al., LIGO-G1400961
Abernathy, LIGO-G1500109]

Mode	Frequency	Q	δQ	R_{shear}	R_{bulk}
BF	2773 Hz	1.14×10^{6}	2.5×10^{3}	9.93×10^{-3}	6.58×10^{-4}
DH	4178 Hz	8.70×10^{5}	2.6×10^{4}	6.85×10^{-3}	4.79×10^{-3}
Hex	6307 Hz	9.32×10^{5}	3.2×10^{4}	9.37×10^{-3}	9.65×10^{-4}
DDH	9707 Hz	9.16×10^{5}	3.8×10^{3}	7.68×10^{-3}	3.62×10^{-3}
Oct	10943 Hz	8.87×10^{5}	1.6×10^{4}	9.05×10^{-3}	1.18×10^{-3}

ϕ_B, ϕ_S Measured

[Harry et al., LIGO-G1400961]

(LMA Titania doped Tantala)

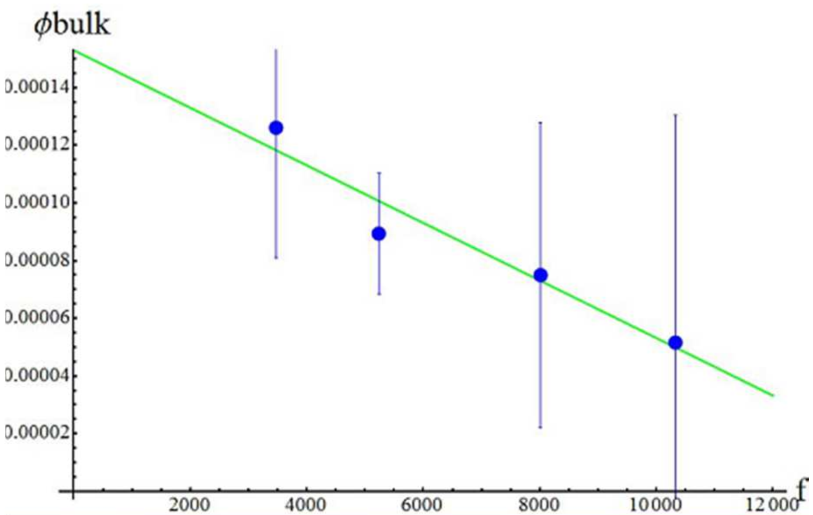

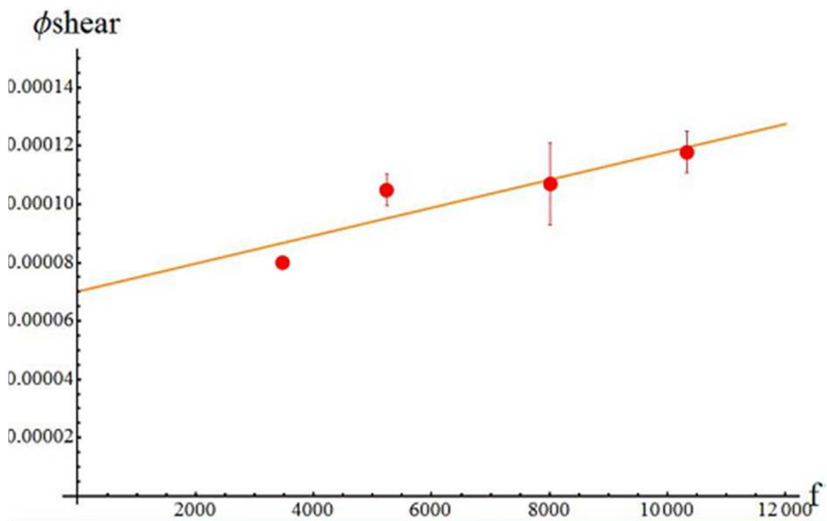

Fits:

$$\phi_B = 1.5\ 10^{-4} - 1.0\ 10^{-8} f$$

$$\phi_S = 7.0\ 10^{-5} - 4.8\ 10^{-9} f$$

$\Rightarrow$ $\phi_B / \phi_S \approx 2$

Elastic Moduli – Conversion Table

Linear homogeneous isotropic elastic response can be described in terms of *any pair* of (complex) elastic moduli chosen among *E* (Young), υ (Poisson), *K* (bulk), *G* (shear), *M* (longitudinal), and λ (1^{st} Lame').

Good sense recipe:
use (hopefully more accurate) measured complex Bulk & Shear moduli in *usual* (Harry's) coating noise formula based on Y (aka, E) and σ (aka, ν) ...

Purple (resp., red) arrows show how to get (*E*,υ) from (*K*,*G*) (resp., (*K*,*G*) from (*E*,υ)) .

	$K=$	$E=$	$\lambda=$	$G=$	$\nu=$	$M=$
$(K,\,E)$	K	E	$\frac{3K(3K-E)}{9K-E}$	$\frac{3KE}{9K-E}$	$\frac{3K-E}{6K}$	$\frac{3K(3K+E)}{9K-E}$
$(K,\,\lambda)$	K	$\frac{9K(K-\lambda)}{3K-\lambda}$	λ	$\frac{3(K-\lambda)}{2}$	$\frac{\lambda}{3K-\lambda}$	$3K-2\lambda$
$(K,\,G)$	K	$\frac{9KG}{3K+G}$	$K-\frac{2G}{3}$	G	$\frac{3K-2G}{2(3K+G)}$	$K+\frac{4G}{3}$
$(K,\,\nu)$	K	$3K(1-2\nu)$	$\frac{3K\nu}{1+\nu}$	$\frac{3K(1-2\nu)}{2(1+\nu)}$	ν	$\frac{3K(1-\nu)}{1+\nu}$
$(K,\,M)$	K	$\frac{9K(M-K)}{3K+M}$	$\frac{3K-M}{2}$	$\frac{3(M-K)}{4}$	$\frac{3K-M}{3K+M}$	M
$(E,\,\lambda)$	$\frac{E+3\lambda+R}{6}$	E	λ	$\frac{E-3\lambda+R}{4}$	$\frac{2\lambda}{E+\lambda+R}$	$\frac{E-\lambda+R}{2}$
$(E,\,G)$	$\frac{EG}{3(3G-E)}$	E	$\frac{G(E-2G)}{3G-E}$	G	$\frac{E}{2G}-1$	$\frac{G(4G-E)}{3G-E}$
$(E,\,\nu)$	$\frac{E}{3(1-2\nu)}$	E	$\frac{E\nu}{(1+\nu)(1-2\nu)}$	$\frac{E}{2(1+\nu)}$	ν	$\frac{E(1-\nu)}{(1+\nu)(1-2\nu)}$
$(E,\,M)$	$\frac{3M-E+S}{6}$	E	$\frac{M-E+S}{4}$	$\frac{3M+E-S}{8}$	$\frac{E-M+S}{4M}$	M
$(\lambda,\,G)$	$\lambda+\frac{2G}{3}$	$\frac{G(3\lambda+2G)}{\lambda+G}$	λ	G	$\frac{\lambda}{2(\lambda+G)}$	$\lambda+2G$
$(\lambda,\,\nu)$	$\frac{\lambda(1+\nu)}{3\nu}$	$\frac{\lambda(1+\nu)(1-2\nu)}{\nu}$	λ	$\frac{\lambda(1-2\nu)}{2\nu}$	ν	$\frac{\lambda(1-\nu)}{\nu}$
$(\lambda,\,M)$	$\frac{M+2\lambda}{3}$	$\frac{(M-\lambda)(M+2\lambda)}{M+\lambda}$	λ	$\frac{M-\lambda}{2}$	$\frac{\lambda}{M+\lambda}$	M
$(G,\,\nu)$	$\frac{2G(1+\nu)}{3(1-2\nu)}$	$2G(1+\nu)$	$\frac{2G\nu}{1-2\nu}$	G	ν	$\frac{2G(1-\nu)}{1-2\nu}$
$(G,\,M)$	$M-\frac{4G}{3}$	$\frac{G(3M-4G)}{M-G}$	$M-2G$	G	$\frac{M-2G}{2M-2G}$	M
$(\nu,\,M)$	$\frac{M(1+\nu)}{3(1-\nu)}$	$\frac{M(1+\nu)(1-2\nu)}{1-\nu}$	$\frac{M\nu}{1-\nu}$	$\frac{M(1-2\nu)}{2(1-\nu)}$	ν	M

Note : the real and imaginary parts of the Poisson moduli σ may have *any sign.*

$$S = \pm\sqrt{E^2 + 9M^2 - 10EM}$$
$$R = \sqrt{E^2 + 9\lambda^2 + 2E\lambda}$$

Ringdown Fitting Residuals

Typical loss angle fitting residuals, TNI measure-ments

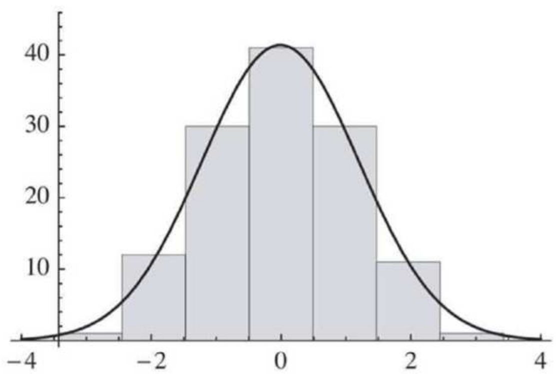

[Villar et al., PRD 81 (2010)]

Typical loss angle fitting residual, clamped cantilever based ring-down measurement

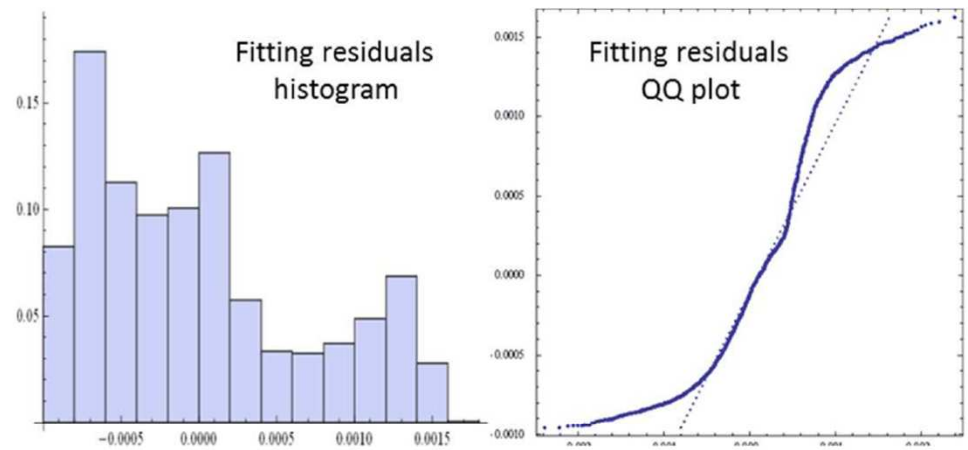

[data courtesy N. Morgado (2008)]

Confidence intervals must be robustly estimated in the non Gaussiann case.

Measuring Thermo-Optic Coefficients

Further coating thermal noise sources stem from thickness and index fuctuations driven by temperature fluctuations of thermodynamic (thermooptic noise) or beam intensity related (photothermal noise) origin.

Coherent superposition of TE and TR fluctuations lead to quasi-cancellation in Silica/Tantala coatings.

Both TE and TR coeffs. are large in crystalline coating. Precise knowledge needed to exploit cancellation by proper design.

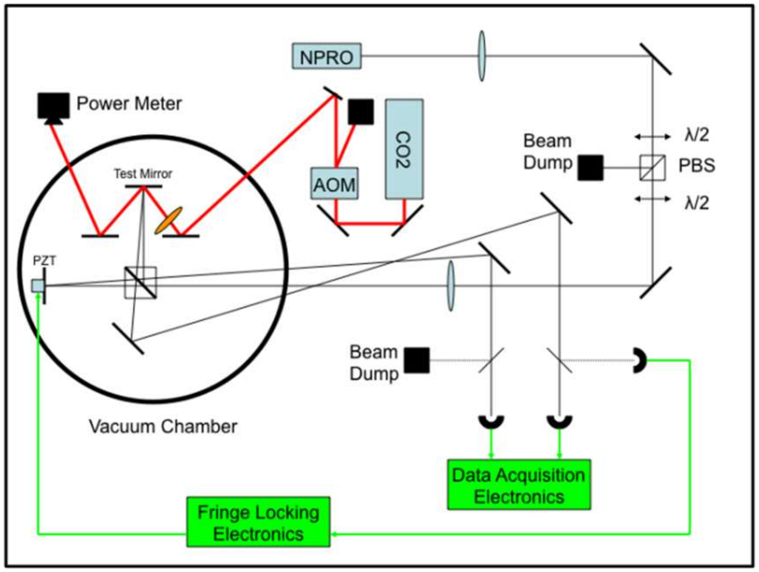

Existing facilites:

- **Whitman College (G. Ogin)**

[Ogin et al., LIGO-P1600067]

Measuring Optical Absorption

Need to measure optical absorption at sub-ppm level, below what is allowed by std ellipsometry. A few groups worldwide have adequate facilities, including

- **Stanford (M. Fejer)**
- **Glasgow (I. Martin)**
- **LMA (G. Cagnoli)**

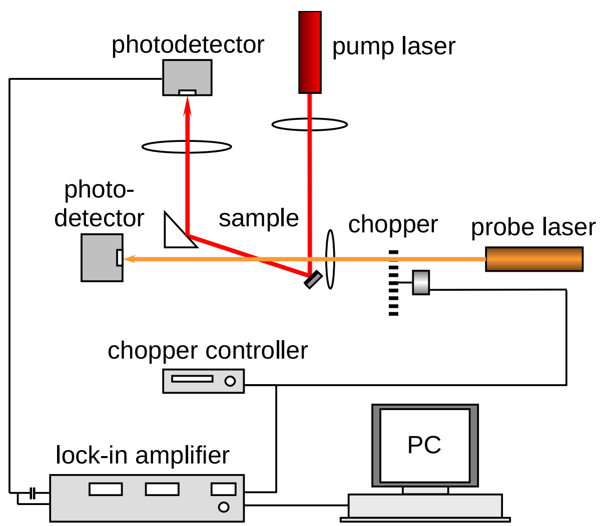

- Photo-thermal Common-path Interferometry (PCI)
  - Measures bulk and coating absorptions
  - Cryo operation possible (15K)
  - Measures thermal lensing due to absorption
  - Sensitivity level (9 W beam): 0.05 ppm/cm (coating), 0.2 ppm/cm and (bulk)

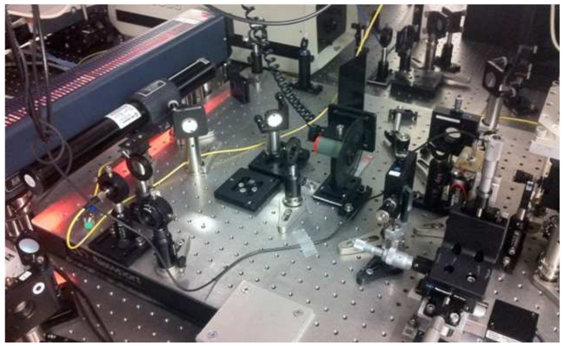

[Lasztka e al., Appl. Opt. 49 (2010) 5391]

Outlook

Why Coating R&D
Where are we now : the aLIGO mirrors

How can we progress:
- Improving Modeling
- Improving Processes
- Improving Characterization

Ongoing Studies & New Ideas:
- Nanolayered Composites
- Silicon Nitrides
- Crystalline Coatings
- M-ary Coatings
- Metamaterial Coatings

Conclusions

Nanolayered Composites

Seminal work on ***thin – layer Titania*** films by Sankur & Gunning [J. Appl. Phys. 66 (1989) 4747]

"Thinner layers (< 250 Å) required higher temperatures [to crystallize]. 65 Å layer films exhibit diffraction only after annealing at 600°C."

➡ ***"Grain size, as deduced from diffraction line broadening, was comparable to the layer thickness"***

"Thicker layers remain in the Anatase phase and never transform into Rutile, even for prolonged (72 h) annealing at the highest temperature s (1100°C). Thinner layers (65 Å) convert into Rutile starting at 900°C"

➡ ***"Below a certain critical thickness crystalli-zation in pure TiO_2 films is inhibited"***

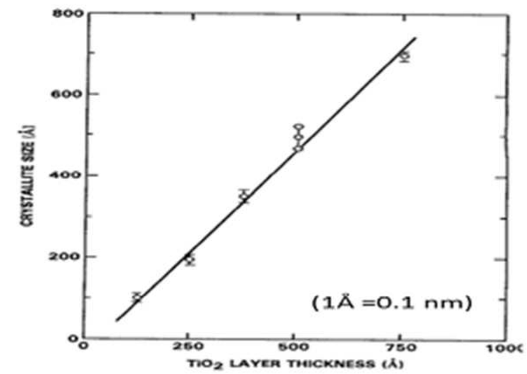

[Gluck et al., J. Appl. Phys. 69 (1991) 3037]

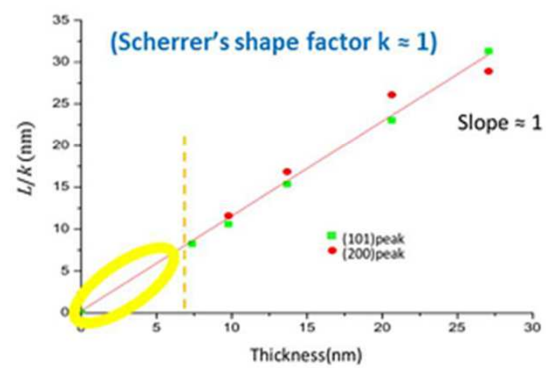

[S. Chao et al., LIGO-G1300921]

Nanolayered Composites

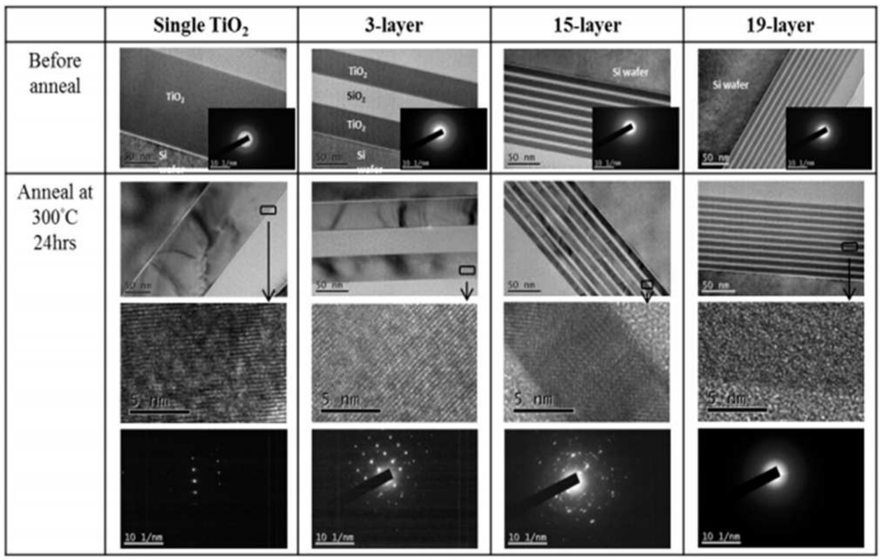

All nanolayered composite prototype films :
$n_{eff} = 2.065$, QWL thick @1064nm

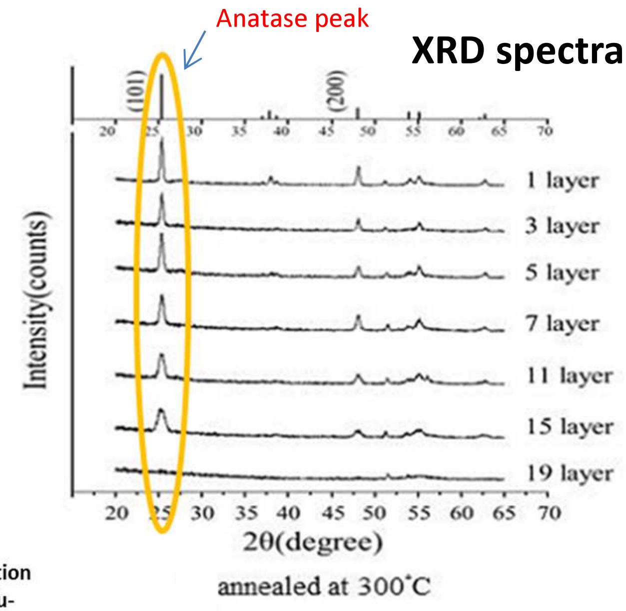

EDXRD investigation of interfacial diffusion before/after annealing (negligible)

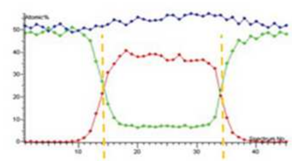

[Pan et al., Opt. Expr. **22** (2014) 29847]

Nanolayered Composites

Loss angle of nm-layered composites reduces upon annealing (before crystallization) .
Losses of annealed composite better than those of Ti doped Tantala (with same *n*)

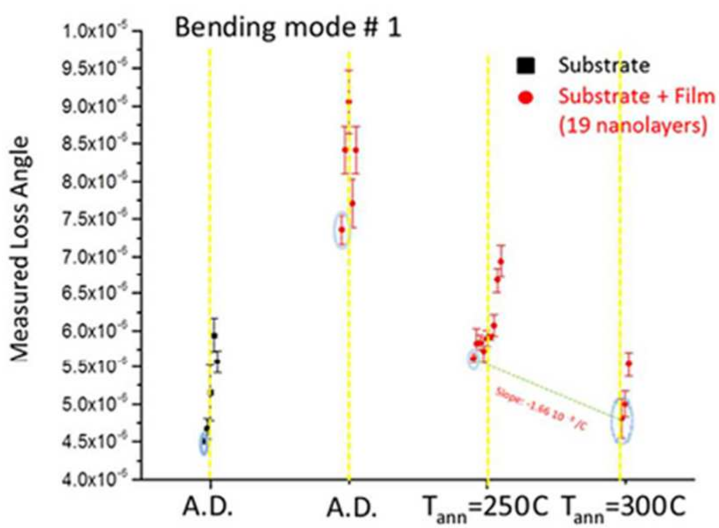

	Loss Angle	
T_{ann}	μ	σ/μ
A.D.	7.36 10^{-6}	0.082
250	5.64 10^{-6}	0.074
300	4.81 10^{-6}	0.074
substrate + film (19 layers)		

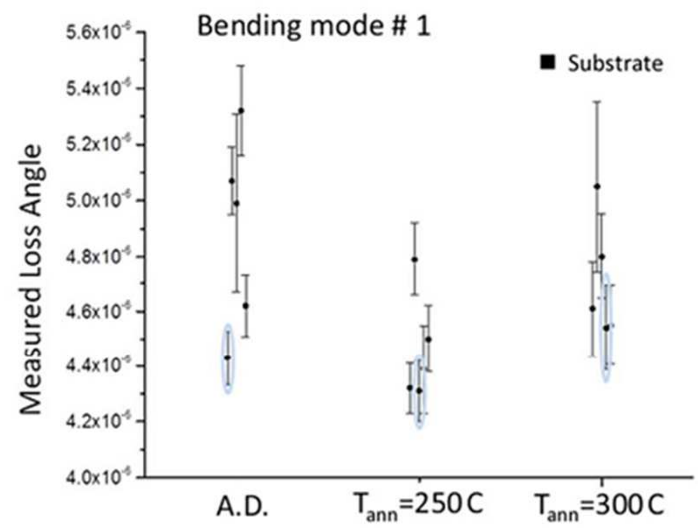

	Loss Angle	
T_{ann}	μ	σ/μ
A.D.	4.48 10^{-6}	0.073
250	4.32 10^{-6}	0.044
300	4.55 10^{-6}	0.046
substrate only (Silicon)		

[Chao et al., LIGO G1401055

Nanolayered Composites

As a byproduct of nanolayered composite resarch, we confirmed the absence of a sensible cryopeak in Titania, much like in Hafnia.

[Chao et al, LIGO-G1601703]

Titania (TiO_2)

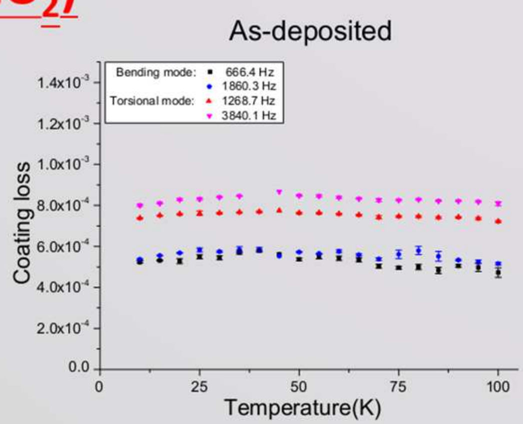

- Coating method: In-house IBS
- There is no cryogenic peak.
- Loss angle is nearly constant with respect to temperature.

Nanolayering makes It is possi-ble to synthetize a variety of low loss, cryofriendly, crystal-lization resistent nanocompo-site materials with an index ragning from 1.58 to 2.33.

What remains TBD

- **Optical loss measurement**
- **Effect of (many) interfaces on optical scattering**
- **How thin can nanolayers be ?**

Nanolayered Composites

Nanometer-layered **Hafnia (12nm)/Alumina (3nm) composites *do not* crystallize upon annealing, up to temperatures of 800 °C**

[M. Liu et al., Appl. Surf. Sci. 252 (2006) 6206].

"XRD analysis shows that the films remain amorphous up to an annealing temperature of 800 °C"

"FTIR indicates that no interface layer forms during annealing up to 800 °C"

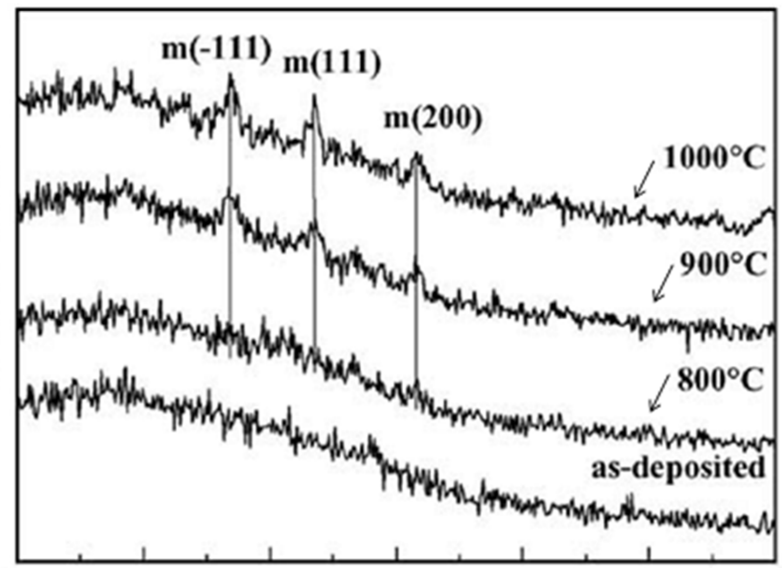

Outlook

Why Coating R&D

Where are we now : the aLIGO mirrors

How can we progress:

- Improving Modeling
- Improving Processes
- Improving Characterization

Ongoing Studies & New Ideas:

- Nanolayered Composites
- **Silicon Nitrides**
- Crystalline Coatings
- M-ary Coatings
- Metamaterial Coatings

Conclusions

Silicon Nitrides

- SiN_x obtained from PECVD.
- **Stoichiometry depends on deposition params** (gas flow rate, substrate temperature (x ranging from 0.40 to 0.87). Larger x $\rightarrow$ larger stresses in the film (120-420 Mpa). Higher stress $\rightarrow$ lower mechanical losses (reduces TLS, and phonon coupling to them).
- **Refractive index can be fine tuned between 1.8 and 2.6. Can be used for both low and high index material).**
- **Mechanical loss angle at $\sim 10^2 Hz$ below 10^{-5}; improves at cryo-temperatures. Extinction coefficient below 10^{-3}.**

[Chao, Proc. Proc. OSA-OIC 2016, paper MB.12]

Silicon Nitrides, contd.

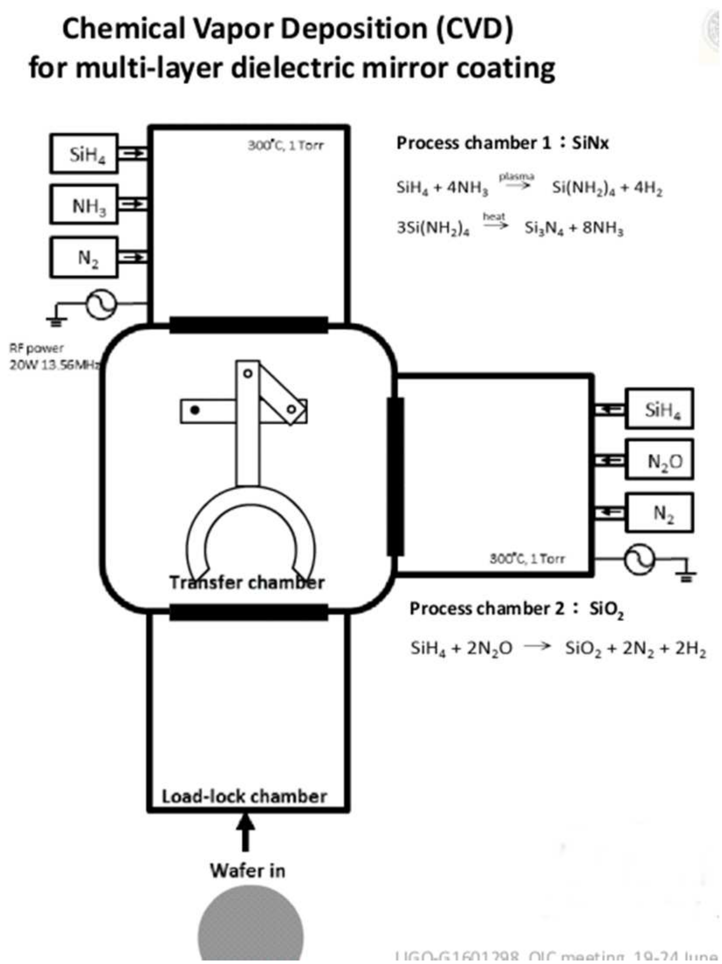

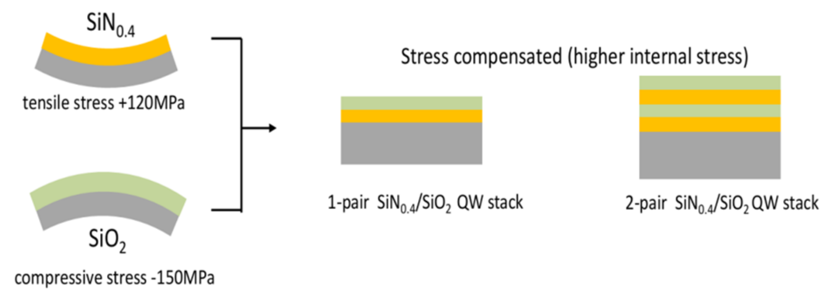

SiN0.4 /SiO2 QW pairs deposited by all-CVD process show room temperature mechanical loss $\sim 10^{-5}$, lower than Ta_2O_5 -TiO2 /SiO_2 in current GW detector.

	2-layer	4-layer
High stress (measured)	$(4.42 \pm 1.83) \times 10^{-5}$	$(9.28 \pm 0.55) \times 10^{-5}$

[Chao et al, LIGO G1601298]

Outlook

Why Coating R&D

Where are we now : the aLIGO mirrors

How can we progress:

- Improving Modeling
- Improving Processes
- Improving Characterization

Ongoing Studies & New Ideas:

- Nanolayered Composites
- Silicon Nitrides
- Crystalline Coatings
- M-ary Coatings
- Metamaterial Coatings

Conclusions

Crystalline Coatings (GaAs/AlGaAs, GaP, AlGaP)

- GaAs/AlGaAs - Strain noise level may be reduced by a factor ~3 compared to current aLIGO; no cryo peak; better at lower T [Cole et al., Nat. Phot. 7 (2013) 644]. Very low optical (absorption & scattering) losses (at ppm lev- els for aLIGO design) [Cole et al., Optica 3 (2016) 647; see also Steinlechner et al., LIGO-G1401032; Singh, LIGO-G1501132]. Must be transferred & bonded to substrate.

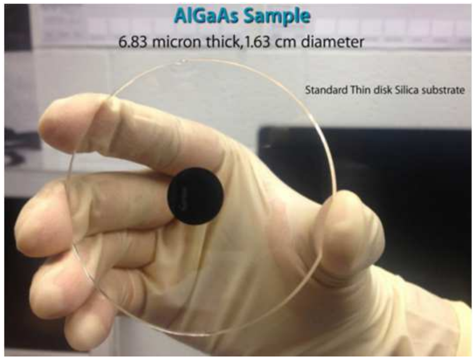

- GaP/AlGaP - Coating *lattice-matched to crystalline Silicon* test mass (→ operation @1550nm) [Lin et al., Opt. Mater. Express, 5 (2015) 1890] Strain noise level reduced by a factor ~5 compared to current aLIGO; no cryo peak [Cumming et al., CQG 32 (2015) 035002]. Unsuitable for room temperature operation (large TE noise

Both GaAs/AlGaAs and GaP/AlGaP

Technology Challenges

- Insufficient size for MBE grown c-coatings (as of today).
  - Upscaling (GaP/AlGaP) to ~ 40cm ⌀ ?
  - Tiling (GaAs/AlGaAs) → Adhesion issues, curvature; edge scattering ?
- *oval defects* observed in MBE grown films → scattering ?

  [Szerling et al. , Opt. Appl. XXXV (2005) 537]

Modeling Issues (poorly investigated so far)

- AlGaAs and AlGaP are III-V compounds w. cubic cell ("zinc-blende") → optical & viscoelastic *anisotropy*
- Nonlinear optical (Pockels, Kerr, free-carrier) effects

} Impact on noise ?

[Abernathy et al. LIGO T1400340; T1400276, T1500268, T1500357]

Outlook

Why Coating R&D

Where are we now : the aLIGO mirrors

How can we progress:

- Improving Modeling
- Improving Processes
- Improving Characterization

Ongoing Studies & New Ideas:

- Nanolayered Composites
- Silicon Nitrides
- Crystalline Coatings
- ➡ M-ary Coatings
- Metamaterial Coatings

Conclusions

Ternary (m-ary) Coatings

[Steinlechner et al., PRD 91 (2015) 069904]
[Yam et al., PRD 91 (2015) 042002]

Use optically dense(r) but lossy-(er) materials in the bottom layers, where field is weak(er).

Fewer doublets;
Thinner coating , lower TN

TBD
- Thickness optimization;
- Effect on spectral response of different material chromatic dispersion ;

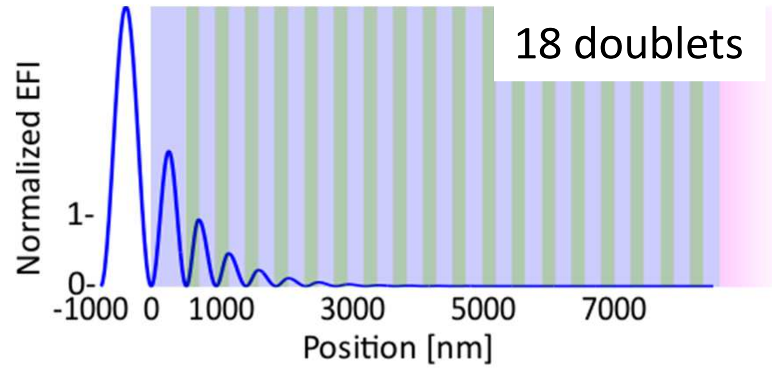

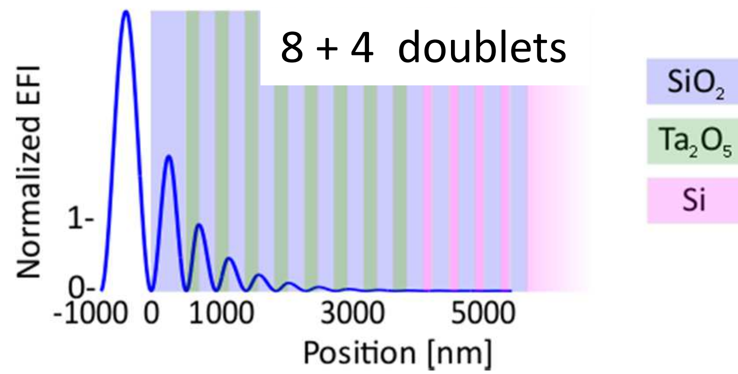

[20% TN reduction at 25C]

Outlook

Why Coating R&D

Where are we now : the aLIGO mirrors

How can we progress:

- Improving Modeling
- Improving Processes
- Improving Characterization

Ongoing Studies & New Ideas:

- Nanolayered Composites
- Silicon Nitrides
- Crystalline Coatings
- M-ary Coatings
- ➡ Metamaterial Coatings

Conclusions

Mie MM Mirror

In the spectral bands where the permeability *or* the permittivity of the Mie MM is negative (*not* both), the effective characteristic impedance of the composite is imaginary ($Z = \iota X$, *pure reactance*), as well as its propagation constant ($\beta = -\iota|\beta|$, *evanescent wave*).

Under such circumstances, the reflectance of a Mie-MM-filled halfspace is

$$R = \left|\frac{\iota X - Z_0}{\iota X + Z_0}\right|^2 = 1$$

and the extinction length in it is $|\beta|^{-1}$.

➡ **Ideally, the above properties could allow to design a *perfect* ($R = 1$) *and thin* ($|\beta| \gg 1$) mirror ...**

Example (Numerical)

Numerical simulation (CST© commercial code)

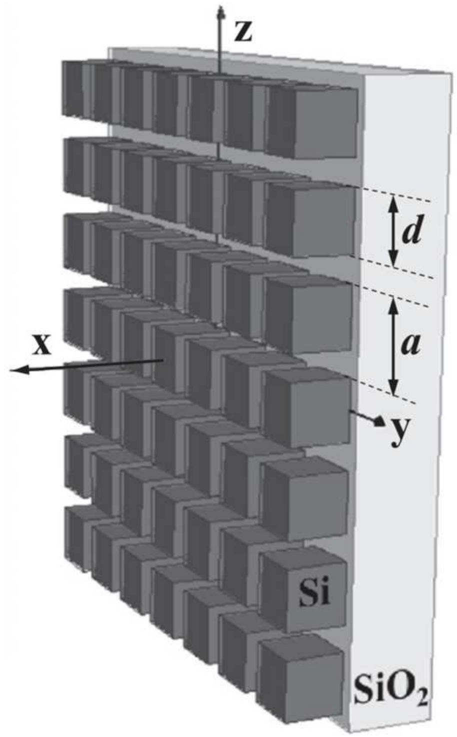

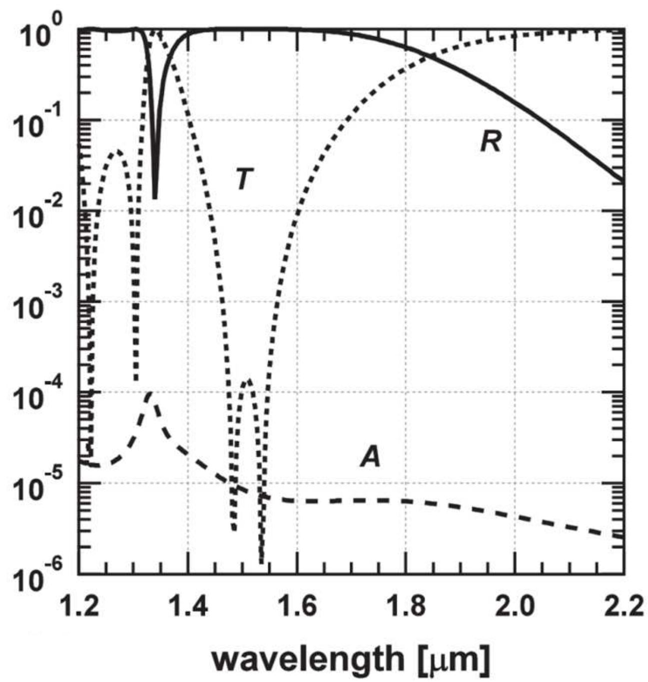

Silicon on Siica
(losses included)

$$d = 450\,nm$$
$$a = 670\,nm$$

Transmittance
& absorbance
below 10^{-5}

[Slovick et al., Phys. Rev. B88 (2013) 165116]

Mie-MM Mirror Feasibility (2017)

Best method as of 2017 in terms of accuracy in nanoparticle (nano-cylinder) size /placement

- e-beam lithography
- reactive-ion etching
- filler deposition

Silicon on Silica or Alumina; Si_3N_4 filler

[Staude et al., ACS nano, 7 (2013) 7824]

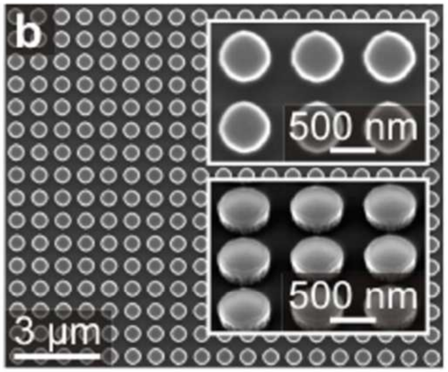

Electron microscopy Image of prototype [Staude, et al.]

⋮

Cheapest (and worst in terms of process control)

- Colloidally self-assembly mask
- ...

[Chang et al., ACS Nano Lett. 11 (2011) 2533]

➡ **Scalability poses no problem**

See e.g. [Krasnok et al., Proc. SPIE 9502 (2015) 950203] for a review

More Coating R&D

keyword	year	selected reference(s)	Status
Thickness Optimization	2005	LIGO G050176 (2005) ... PRD 81 (2010) 122001	*AdLIGO baseline design*
Doped Tantala	2007	Class. Quantum Grav. 24 (2007) 405 ...	*AdLIGO baseline design*
Cryogenic Coatings	1999	Int. J. Mod. Phys. D8 (1999) 557 ... Opt. Lett. 38(2013) 5268	R&D
"Wide" (or HOGL) beams	2003	PRD 67 (2003) 102004 ... CQG 30 (2013) 035004	R&D
Khalili's Resonator and "Etalon"	2004	Phys. Lett. A334 (2004) 67, Phys. Lett. A375 (2011) 4147	R&D
Coating-less Mirrors	2004	Phys Lett A324 (2004) 345,..., PRD 76 (2007) 053810	R&D
Diffractive "Mirrors"	2006	CQG 23 (2006) 7297 ... LIGO P-1300034 (2013)	R&D
Crystalline Coatings	2012	LIGO G1200948 (2012) ... Nature Phot. 7 (2013) 644	R&D

So far, only doped Tantala and thickness-optimization progressed to the production stage (and became part of the AdLIGO baseline design).

Most of the above (clever) ideas are still facing *major technological challenges*.

Will nm-layered composites be a viable route ?

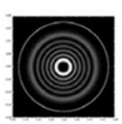

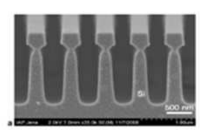

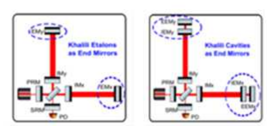

Outlook

Why Coating R&D
Where are we now : the aLIGO mirrors

How can we progress:

- Improving Modeling
- Improving Processes
- Improving Characterization

Ongoing Studies & New Ideas:

- Nanolayered Composites
- Silicon Nitrides
- Crystalline Coatings
- M-ary Coatings
- Metamaterial Coatings

➡ Conclusions

Conclusions

Reducing coating thermal noise is mandatory to improve the performance of interferomeric detectors of GW.

We need well understood, reliable, repeatable protocols to measure coating-relevant material parameters;

We need a better understanding/control of *the Physics* behind the coating (noise) properties;

We need to explore in depth better depositions, smart doping, nanolayered composites, M-ary coating; crystal-line coatings and maybe Mie Metamaterials;

We need young talented scientists to work on such issues (and money to keep them alive).

Acknowledgements

This work has been sponsored in part by the EU through the EU-FP-7 ELiTES (IRSES) Project; by the Italian National Institute for Nuclear Physics (INFN, CSN - 5) under the COAT, MidiBRUT and AdCOAT grants; by the National Science Council of Taiwan under NSC-1002221-E-007-099.

Honoring a Master

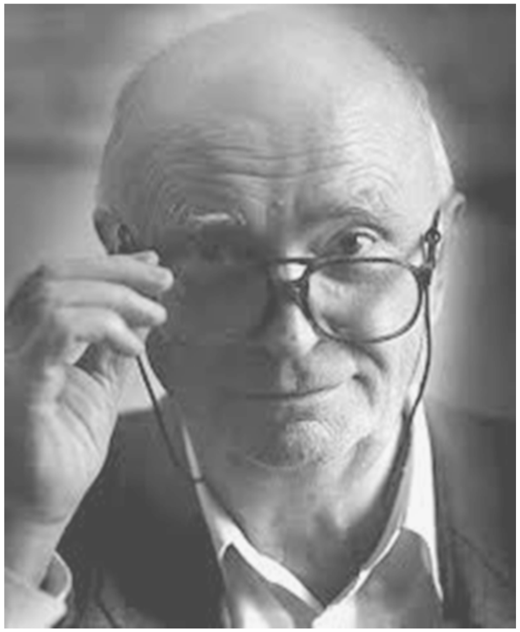

Vladimir Borisovich Braginsky
(3/8/1931-30/3/2016)

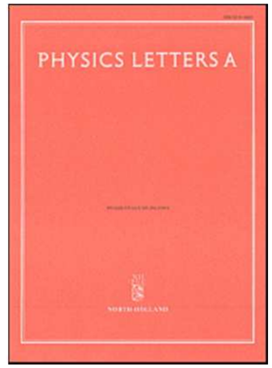

Special Issue:

- Low-dissipation systems,
- Noise and fluctuations,
- Quantum-limited and QND measurements,
- Macroscopic Quantum Mech.,
- Optomechanical effects,
- Optical / microwave whispering gallery modes,
- GW detectors,
- Selected aspects of Gravitation Physics (spin-quadrupole effect, equivalence principle, etc.)

Submission Deadline : March 17th 2017

https://www.journals.elsevier.com/physics-letters-a/call-for-papers/special-issue-in-memory-of-prof-vladimir-borisovich-braginsky

Mie Metamaterials Coatings

Metamaterials (MMs)

From the Greek noun μετά (beyond) is, at large, an artificially engineered material with properties that aren't found in any known natural material.

Historically, meant to denote materials whose dielectric permittivity and/or magnetic permeability is *negative* in some spectral band [Veselago, Sov. Phys. Usp. 10 (1968) 509].

Conceptual extension to mechanical constitutive properties (bulk modulus, density) with applications in Acoustics, Structural Engineering , etc. , followed.

At the core of the US-DoD **Multidisciplinary University Research Initiative** (MURI) , and the UE **Metamorphose** Research Network.

MMs, contd.

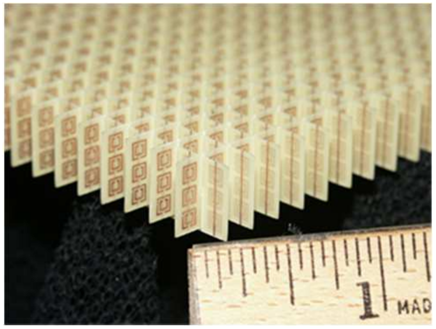

First working metamaterial demonstrated in 2001 [Shelby et al., Science 292 (2001)], based on lattices of split-ring resonators and metallic wires **[Smith et al., PRL 84 (2000) 4184]** wor-king in the GHz range…

Paved the way to unforeseen new apps including e.g. *super-resolution imaging* [Grbic & Eleftheriades PRL 92 (2004) 117403] and *invisibility cloaking* [Shurig et al., Science. 314 (2006) 5801], that were steadily improved during the subsequent decade;

Scaling to optical frequencies initially hindered by large losses in metals; made possible by exploiting Mie resonance in dielectric nanosphere arrays ['O Brien & Pendry, J. Phys. Cond. Matt. 14 (2002) 6383].

Mie MMs in a Nutshell

The spherical multipole expansion of the EM field scattered by a sphere was first derived by Gustav Mie [Ann. Phys. 330 (1908) 377] in terms of spherical Bessel functions.

The scattering coefficients exhibit *resonances,* known as *Mie resonances* [Uslenghi, Electromagnetic Scattering, Acad Press, 1978]

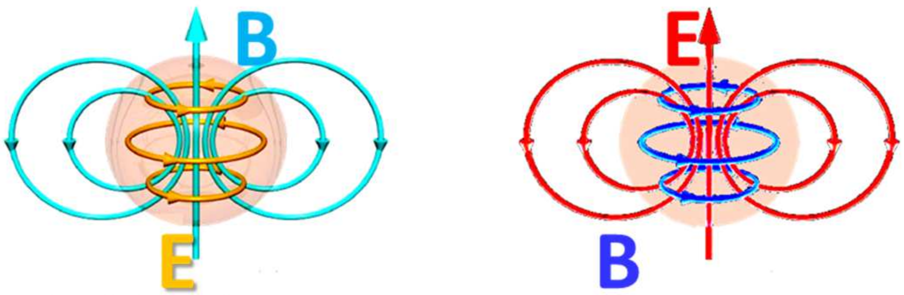

Lowest order (dipole) Mie resonances - Left: magnetic; right: electric

The resonant wavelengths depend on the radius and dielectric contrast of the sphere. For a Si sphere in air, with $d = 0.25\mu$, e.g., the lowest electric and magnetic resonances occur at $\lambda \approx 1.2\mu$ and $\lambda \approx 1.7\mu$

Mie MMs in a Nutshell, contd.

The effective permittivity and permeability of a *lattice of spheres in a host medium* was first computed by Lewin [Lewin, Proc. IEE, 94 (1947) 65]

$$\varepsilon_{eff} = \varepsilon_h \left(1 + \frac{3\eta}{\frac{F(\xi)+2(\varepsilon_h/\varepsilon_S)}{F(\xi)-(\varepsilon_h/\varepsilon_S)} - \eta}\right) \quad , \quad \mu_{eff} = \mu_h \left(1 + \frac{3\eta}{\frac{F(\xi)+2(\mu_h/\mu_S)}{F(\xi)-(\mu_h/\mu_S)} - \eta}\right)$$

where:

η = volume fraction of spheres;

$$F(\xi) = \frac{2(\sin\xi - \xi\cos\xi)}{(\xi^2-1)\sin\xi + \xi\cos\xi}$$

$\xi = \omega\sqrt{\varepsilon_S\mu_S}\, R_S$, R_S = radius of spheres

(ε_h, μ_h) = permittivity & permeab. of host

(ε_S, μ_S) = permittivity & permeab. of spheres

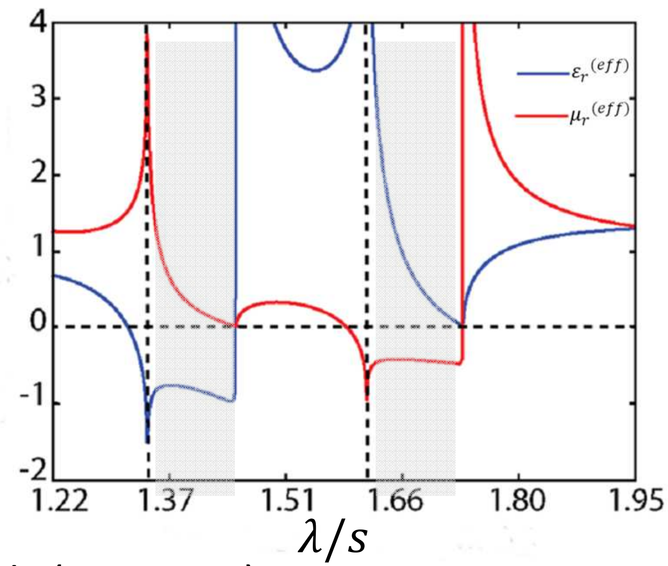

➡ Featuring $Re[\varepsilon] < 0$ *or* $Re[\mu] < 0$ in some bands (*SNG*-MM)

Mie MM Mirror

In the spectral bands where the permeability *or* the permittivity of the Mie MM is negative (*not* both), the effective characteristic impedance of the composite is imaginary ($Z = \iota X$, *pure reactance*), as well as its propagation constant ($\beta = -\iota|\beta|$, *evanescent wave*).

Under such circumstances, the reflectance of a Mie-MM-filled halfspace is

$$R = \left|\frac{\iota X - Z_0}{\iota X + Z_0}\right|^2 = 1$$

and the extinction length in it is $|\beta|^{-1}$.

Ideally, the above properties could allow to design a *perfect* ($R = 1$) *and thin* ($|\beta| \gg 1$) mirror ...

Lossy Mie-MM Mirror

The (normal incidence, plane wave) reflection coefficient of a SNG MM $(Re[\varepsilon]Re[\mu] < 0)$ in vacuum can be written

$$\Gamma = \frac{\frac{Z_{MM}}{Z_0} - 1}{\frac{Z_{MM}}{Z_0} + 1} = \frac{Re[\bar{Z}_{MM}] - 1 + jIm[\bar{Z}_{MM}]}{Re[\bar{Z}_{MM}] + 1 + jIm[\bar{Z}_{MM}]} \qquad R = |\Gamma|^2 = \frac{(Re[\bar{Z}_{MM}] - 1)^2 + (Im[\bar{Z}_{MM}])^2}{(Re[\bar{Z}_{MM}] + 1)^2 + (Im[\bar{Z}_{MM}])^2}$$

For small losses , $|Im[\varepsilon]| \ll |Re[\varepsilon]|$ and $|Im[\mu]| \ll |Re[\mu]|$

$$\bar{Z}_{MM} = \pm\sqrt{\frac{\varepsilon_0}{\mu_0}\left|\frac{Re[\mu]}{Re[\varepsilon]}\right|}\left[j - \frac{\delta}{2}\right], \; \delta = \frac{Im[\varepsilon]}{Re[\varepsilon]} - \frac{Im[\mu]}{Re[\mu]}$$

Hence

$$R = 1 - \frac{2\sqrt{\frac{\varepsilon_0}{\mu_0}\left|\frac{Re[\mu]}{Re[\varepsilon]}\right|}}{1 + \frac{\varepsilon_0}{\mu_0}\left|\frac{Re[\mu]}{Re[\varepsilon]}\right|}|\delta|$$

Can be made small at will using *low-loss dense* materials

Finite Thickness Mie-MM Mirror

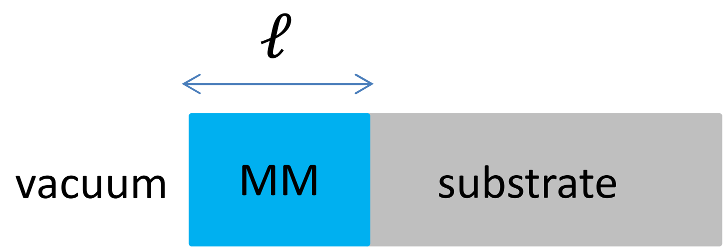

After some lengthy but obvious algebra (reflection coefficient transport equation), under the assumption that both both reflectances $R_{1,2}$ at the vacuum-MM and MM-substrate interfaces are close to unity ,

$$R_{1,2} = 1 - \delta_{1,2}\ , \text{ with } \delta_1 \sim \delta_2 \sim \delta \ll 1$$

It is found that for a finite-thickness MM layer

$$R_\ell = R_\infty - \delta_\ell\ , \text{ with } \delta_\ell \le 2\exp\left(-\frac{4\pi\ell}{\lambda_0}\sqrt{\frac{|Re[\varepsilon]Re[\mu]|}{\varepsilon_0\mu_0}}\right)$$

Example (Numerical)

Numerical simulation (CST© commercial code)

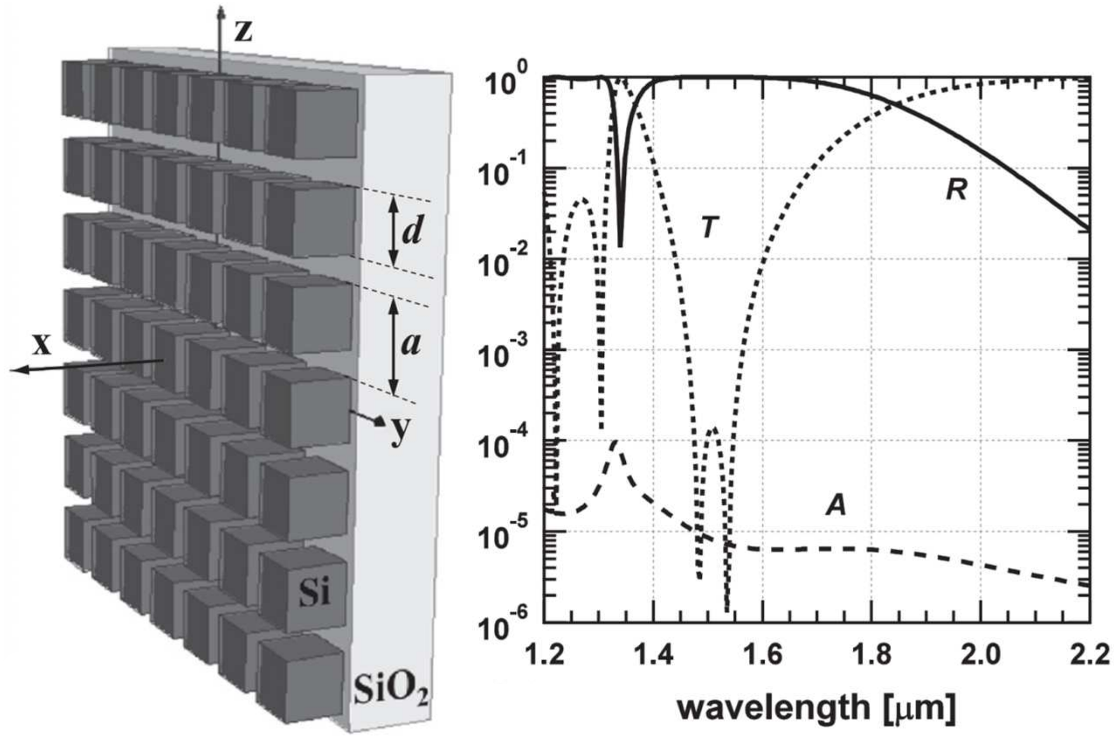

Silicon on Siica
(losses included)

$$d = 450\,nm$$
$$a = 670\,nm$$

Transmittance
& absorbance
below 10^{-5}

[Slovick et al., Phys. Rev. B88 (2013) 165116]

Thermal Noise of MM Coating

For practical purposes, the viscoelastic properties of a Mie-MM can be computed using *effective medium theory* [Principe et al., Phys. Rev. D91 (2015) 022005].

The MM-film can be one order of magnitude thinner than a traditional (multilayer, Bragg) coating with equivalent reflectance. We may naively expect a comparable ratio (one order of magnitude) in thermal noise PSD.

A rigorous ab-initio thermal noise calculation can be worked out paralleling the analysis in [Heinert et al., Phys. Rev. D88 (2013) 42001] for grating reflectors (Pinto et al., work in progress).

Mie-MM Mirror Feasibility (2017)

Best method as of 2017 in terms of accuracy in nanoparticle (nano-cylinder) size /placement

- e-beam lithography
- reactive-ion etching
- filler deposition

Silicon on Silica or Alumina; Si_3N_4 filler

[Staude et al., ACS nano, 7 (2013) 7824]

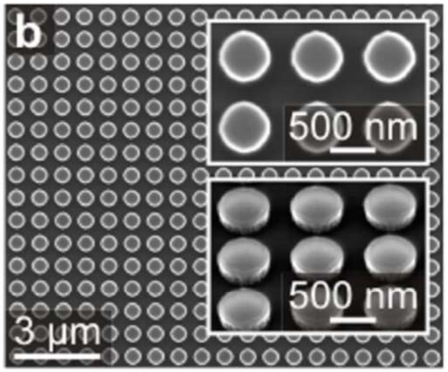

Electron microscopy Image of prototype [Staude, et al.]

⋮

Cheapest (and worst in terms of process control)

- Colloidally self-assembly mask
- …

[Chang et al., ACS Nano Lett. 11 (2011) 2533]

➡ **Scalability poses no problem**

See e.g. [Krasnok et al., Proc. SPIE 9502 (2015) 950203] for a review

New Ideas May be Hard to Receive … but Worth a Try !